PARTICLE DYNAMICS MODEL FOR HURRICANE EVACUATION AND FUEL SHORTAGE: MODEL BASED POLICY ANALYSIS

FINAL REPORT

JUNE 2019

Sirish Namilae & Dahai Liu

US DEPARTMENT OF TRANSPORTATION GRANT 69A3551747125

DISCLAIMER

The contents of this report reflect the views of the authors, who are responsible for the facts and the accuracy of the information presented herein. This document is disseminated under the sponsorship of the Department of Transportation, University Transportation Centers Program, in the interest of information exchange. The U.S. Government assumes no liability for the contents or use thereof.

1. Report No.	2. Government Accession No.	3. Recipient's Catalog No.
4. Title and Subtitle PARTICLE DYNAMICS MODEL FOR HURRICANE EVACUATION AND FUEL SHORTAGE: MODEL BASED POLICY ANALYSIS		5. Report Date June 2019 6. Source Organization Code
7. Author(s) Sirish Namilae, Dahai Liu		8. Source Organization Report No.
9. Performing Organization Name and Address Center for Advanced Transportation Mobility Transportation Institute 1601 E. Market Street Greensboro, NC 27411		10. Work Unit No. (TRAIS) Contract or Grant No. 69A3551747125 Sub contract: **270128E**
11. Sponsoring Agency Name and Address University Transportation Centers Program (RDT-30) Office of the Secretary of Transportation–Research U.S. Department of Transportation 1200 New Jersey Avenue, SE Washington, DC 20590-0001		12. Type of Report and Period Covered Final Report: March 2018 to June 2019 13. Sponsoring Agency Code USDOT/OST-R/CATM
14. Supplementary Notes:		

15. Absract

The purpose of this study is to examine the various factors that affect fuel shortage during hurricane evacuation and develop strategies to mitigate it. Fuel Shortage during hurricane Irma is modelled as contagion. We use the data accumulated by Gasbuddy, a free crowd sourced data application, and employ parameter identification technique to optimally estimate various characteristics exhibited by a contagion. We then develop a method to deterministically reproduce the real-life data using differential equations to apply optimal control theory. Using this approach, we are able to develop a time optimal refueling strategy for empty fuel stations that help reduces fuel shortage with resource scarcity as a constraint. We find that there is significant relationship of the contagion like behavior of different areas and cities with their distance from hurricane landfall, population and number of operating automobiles in these places. This is evident with Miami/Ft Lauderdale area having an R0 value of 5.54 compared to Orlando, with a R0 value of 1.93.

16. Key Words	17. Distribution Statement
Evacuation, Fuel shortage, Modeling	Unrestricted; Document is available to the public through the National Technical Information Service; Springfield, VT.

18. Security Classif. (of this report)	19. Security Classif. (of this page)	20. No. of Pages	21. Price
Unclassified	Unclassified	80	…

Form DOT F 1700.7 (8-72) Reproduction of completed page authorized

TABLE OF CONTENTS

EXECUTIVE SUMMARY

For the past couple of hurricane seasons, fuel shortage has been a recurring predicament. The purpose of this study is to examine the various factors that affect fuel shortage during hurricane evacuation and develop strategies to mitigate it. Fuel Shortage during hurricane Irma is modelled as contagion. We use the data accumulated by Gasbuddy, a free crowd sourced data application, and employ parameter identification technique to optimally estimate various characteristics exhibited by a contagion. We then develop a method to deterministically reproduce the real-life data using differential equations to apply optimal control theory. Using this approach, we are able to develop a time optimal refueling strategy for empty fuel stations that help reduces fuel shortage with resource scarcity as a constraint. We find that there is significant relationship of the contagion like behavior of different areas and cities with their distance from hurricane landfall, population and number of operating automobiles in these places. This is evident with Miami/Ft Lauderdale area having an R_0 value of 5.54 compared to Orlando, with a R_0 value of 1.93. We also find that by the inclusion of an optimal refueling strategy modeled as vaccination for the fuel shortage SIR model, helped reduces fuel shortage and also control it by reducing the maximum number of inoperative fuel stations in any given area. Also using bilinear interpolation, we were able to show the best-case scenario of optimal refueling strategy that can be obtained for a given city/area. We also developed an agent based model simulation to study the refueling capabilities of fuel stations at an exit on a busy interstate during the event of a hurricane.

CHAPTER 1. EPIDEMIC MODEL FOR HURRICANE EVACUATION AND FUEL SHORTAGE

Introduction

Recent hurricanes in Southeast United States have led to mass evacuations. During hurricane Irma in 2017, 23 counties in Florida issued mandatory evacuation orders, with the remaining 44 counties putting in place voluntary orders. Analysis of hurricane Irma traffic data obtained from Florida Department of Transportation (FDOT) indicates a net exodus of 550,000 vehicles from the southern parts of Florida. It is estimated that approximately 6.8 million Floridians and tourists took to the roads in the days leading up to the storm [1]. Such mass evacuations have also been observed during hurricane Florence [2], affecting North and South Carolinas as well as during hurricane Michael [3]. Hurricane evacuees tend to make longer, intercity trips to stay with friends and family outside the impacted area and to completely move out of the storm path [4]. The high-volume mass evacuations, disruptions to the supply chain, long distances travelled, and fuel hoarding from non-evacuees have led to localized fuel shortages lasting several days and a cascade of problems. For example, the large-scale evacuation during hurricane Irma created a widespread fuel shortage problems days before the hurricane's landfall for most of Florida and especially for south Florida. The fuel shortage problems gave rise to various other issues such as an unpredictable increase in fuel prices that exasperate and hinder evacuees living on low wage income, traffic congestion on the highways and increased traffic flow, particularly in rural areas [5]. After the hurricane passage, delays in recovering power also affected the fuel situation and emergency transportation needs, for e.g. getting medical supplies and power to hospitals [6]. During

evacuations, fuel shortages result in stranded cars and exacerbate traffic problems in an emergency situation. Understanding the characteristics of fuel shortage during hurricane evacuation is crucial to the mitigation of this problem and reducing the casualties caused by an imminent hurricane.

The progression of fuel shortage through a geographic area and the return to normal fuel supply has similarities with the spread of infectious diseases. Sociologists and computational scientists have long studied such events using biological models of infectious disease spread. Modeling interconnected social events as contagion leads to the analysis of these events in a new light. For example, contagious disease modelling has also been used to study social phenomena that show epidemic like behavior, such as Election campaign donations [7], spread of emotional influence in social media [8], adoption process, suicidal ideation [9] and the likelihood of increase of exercisers depending on level of activeness of their peers [10]. The social contagion of altruism, i.e. the effect of one person's behavior on the group's generous behavior was examined by Tsvetkova and coworkers [11] using epidemic models. A recent study by Towers et al [12] models the epidemic behavior of mass killing related to gun violence. The study reported that the likelihood of another mass killing increased because of preceding occurrence of similar events [12] .Feng et al, also proposed a contagion model that take into consideration the effect of "duel contagions" [13], where they study the spread of a biological phenomenon (influenza) affecting a social phenomenon (flu vaccination and influence of social media in spreading news about vaccination). Similarly, Towers and coworkers [14], model the spread of public panic as a social contagion, following the first imported case of Ebola into the United States in 2014. The study found that the social contagion in this case outgrew the actual biological contagion of Ebola virus

and was the main cause of public outcry. Sprague [15], studied the use of complex contagion models compared to “simple” contagion models to examine behavioral ‘fads’ in social media. These studies suggest that epidemiological models are quite successful in not only examining and predicting of disease outbreaks, but also to study and model problems that exhibit epidemic like characteristics.

Most, if not all, of these studies focus on how information, trends, behaviors and other entities spread between individuals or populations. This process of spreading an inducing agent is commonly referred as ‘contagion’. For most common cases, the most well studied contagion models are the classic compartmental epidemiological models such as SIS (Susceptible-Infected-Susceptible), SIR (Susceptible-Infected-Recovered) or SIRS (Susceptible-Infected-Recovered-Susceptible), used for studying the spread of microbial diseases [16]-[19]. Compartmental models divide the host population into susceptible, infected and recovered compartments with a set of differential equations describing transition of population into these different compartments [20]. Susceptible hosts or agents are prone to becoming infectious a in given time after exposure [20], [21]. Infectious hosts who are now infected help transmit the infection to the susceptible agents. Recovered or removed agents that have become immune to the infection do not have the ability to transmit the epidemic and consequently have no effect on the transmission dynamics [20], [21]. In the case of fuel shortages during hurricane evacuation, the contagion inducing agent is the traffic flow caused by evacuees.

While news reports have documented fuel shortages during the past hurricanes, crowd-sourced data from the social media platform Gasbuddy [22] has quantified the shortages during recent hurricanes. Our analysis of this crowdsourced data for recent hurricanes

including hurricane Irma, indicates characteristics of an epidemic. For example, a refueling station in the vicinity of another station that is out of gas is more likely to be depleted of fuel soon, similar to an infection transmission. In this study, we apply the SIR dynamics to model fuel shortage during hurricane evacuation as an epidemic and examine the infection dynamics comparing with existing empirical data as shown in the schematic in Figure 1(a). We further apply optimal control theory to determine an optimal refueling strategy utilizing an SIR dynamic model with vaccination, for different resource constraints that determine the amount of control input for the optimal controller shown in the schematic in Figure 1(b).

We utilize the data from the crowd source platform Gasbuddy for modeling the fuel-shortage epidemic. The unique advantage of this data source is the easy access to on-the-fly data as the evacuation and fuel shortages are evolving. However, there is a difficulty in utilizing continuous differential equations to model this problem. There are fluctuations and discontinuities in the Gasbuddy data, because of the inherent discreteness of information release which leads to waves of evacuation and as consumption. This data pattern makes it difficult to implement the optimal control theory, since the basis of the control theory depends on the dynamics model being made up of continuous ODEs [23], [24]. To address this problem, we use an Unscented-Kalman-Filter algorithm to numerically estimate the different SIR model parameters that characterizes the dynamics of disease transmission. We then utilize these parameters to compute the continuous time invariant SIR data.

We then determine the optimal refueling strategy to mitigate fuel shortage during hurricane evacuation using a bang-bang optimal control methodology [23]. Such control strategies have been developed in the context of infection dynamics for vaccination policy [23], [24]. To the best of our knowledge, this is the first application of the SIR model and the optimal control

algorithms to the problem of fuel shortages during hurricanes. Our aim with the application of the optimal refueling strategy is shown in Figure1(b). This type of modelled approach shows that control of an event modelled as a contagion by an external control input, can also be modeled as part of the system. We utilize the fuel shortage data for hurricane Irma and suggest refueling strategies for specific cities using this approach. The next section deals with the mathematical development of the problem followed by the results and discussions.

Methods

Data Sources

The data pertaining to percentage of fuel stations out of gas, for this study, were acquired from Gasbuddy. Gasbuddy is an online database containing vital roadside information on more than 150,000 fuel stations. The website also provides real-time fuel price information to drivers through a designated mobile app created for both iOS and Android platforms [25]. Along with that, the website also enables existing drivers to report and review various refueling establishments throughout the United States. Gasbuddy played a crucial role during hurricane Irma and Florence by connecting evacuees over their database network to provide real time information on fuel reserves in different affected cities and areas. Using the mobile app, drivers were able to report fuel stations that were out of fuel in affected areas, thus contributing to driver awareness on the road that helped evacuees stay informed and cautious about fuel availability during evacuation [26].

A recent article in The Wall Street Journal reports that the Gasbuddy Mobile app was downloaded 300,000 times during the events leading up to hurricane Irma, compared to 30,000 on a typical day [26]. Florida Governor Rick Scott and Texas congressman Ted Poe both recommended the use of Gasbuddy during hurricane evacuation of the respective states

during hurricane Irma and Harvey. Mr. Doyle, the CEO of Gasbuddy, said that the reliability of the crowdsourced data is ascertained by cross checking fuel price reports with user's location information [26]. A similar study by Levin et al uses data triangulation to acquire volunteered user generated data from multiple distinct sources to ensure credibility and reliability [27].

During the 2017 hurricane Irma, Gasbuddy was able to obtain data about the percentage of refueling stations out of fuel in key cities around the state of Florida. The data represented refueling stations in key Floridian city/areas such as Jacksonville, Orlando, Tampa/St Petersburg Area, Fort Myers/ Naples Area, West Palm and Miami/Fort Lauderdale areas with fuel discrepancies from 9/6/2017 to 9/18/2017.

Data on the number of fuel stations in each city/area were obtained from the United States Census Bureau [28]. For this study, traffic data collected by the Florida Department of Transportation (FDOT) are also used. The traffic data were collected from Telemetered Traffic Monitoring Sites (TTMS) stationed throughout roads and highway statewide. These TTMS points are able to obtain data on the number of vehicles passing every one-hour interval for twenty-four hours [29].

SIR Dynamics for Fuel Shortages

In the SIR model, schematically shown in Figure 1 (a), we treat percentage of refueling stations without gasoline as "infected (I)", percentage of refueling stations with gasoline that are prone to running out of gasoline as "susceptible (S)" and percentage filled with gasoline after running out of fuel as "recovered (R)". The recovered refueling stations do not get re-infected (experience fuel shortage) in this case as the model and the on-ground situation

represents a short-term outbreak. In terms of differential equations, the dynamic model for the SIR is:

$$\frac{dS}{dt} = -\beta S(t)I(t) \quad \textit{Eq. 1}$$

$$\frac{dI}{dt} = \beta S(t)I(t) - \gamma I(t) \quad \textit{Eq. 2}$$

$$\frac{dR}{dt} = \gamma I(t) \quad \textit{Eq. 3}$$

Equation 3 for dR/dt does not affect the dynamics for S(t) and I(t) which stipulates the fact that recovered gas stations do not affect transmission [20].

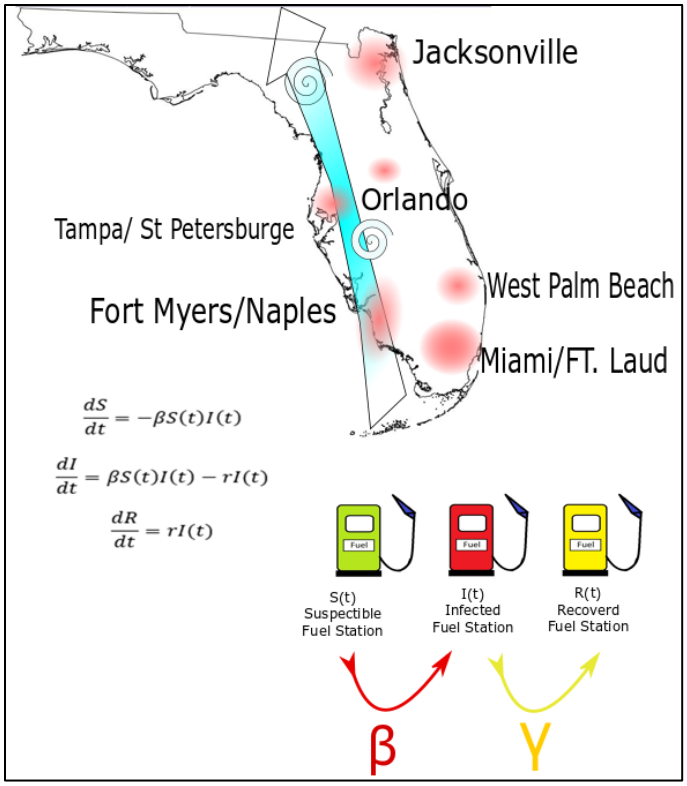

Figure 1(a). SIR dynamics model repurposed for fuel station shortage to study shortage during hurricane evacuation.

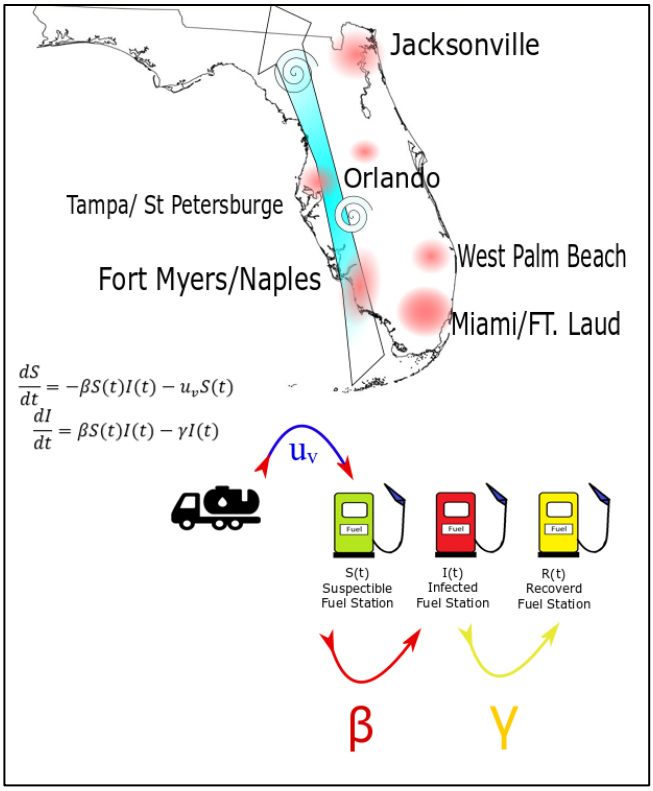

Figure 1(b). SIR dynamics model augmented to include vaccination rate as per capita rate of refueling, u_v.

The parameters β and γ represent the transmission rate per capita and recovery rate, which in the current context represent the rate at which the susceptible refueling stations are emptying and the empty gas stations are resupplied respectively. As in a conventional SIR model the mean infectious period, i.e. period in which most fuel stations are without fuel, is $1/\gamma$. We use the crowdsourced data from the Gasbuddy website in conjunction with Unscented Kalman Filter (UKF) to determine the β and γ parameters. The Kalman Filter provides an effective technique designed to estimate the epidemic parameter with measurement correction from empirical data [21], [30]. Another viable reason for the use of UKF is that crowdsourced data collection potentially leads to a discontinuous data pattern that makes it difficult to implement the optimal control theory, which utilizes continuous ordinary differential equations. The UKF

provides a range of values that can be used to develop a continuous time invariant SIR model that can closely resemble acquired data that do not have any discontinuities. The estimated epidemic parameters are then be correlated to different geographical and demographical data of the cities to gain insight into the factors that influence the fuel shortages.

Parameter estimation

To estimate the epidemic parameters, we set up the process and measurement equations as shown in Eq. 4 through Eq. 9. Using the data from GasBuddy.com for the measurement update in the Unscented Kalman Filter algorithm, we can simultaneously generate the synthetic data for the mechanistic SIR Model and estimate the parameters β and γ. The differential equations of the Fuel Shortage SIR model are then converted to discrete time form at different days, k, using the Euler Method. The state vector that is input into the UKF is defined as

$$X_k = [S_k, I_k, \beta_k, \gamma_k]^T$$

That is the states are susceptible, infected, recovered refueling stations and the parameters β and γ, rates at which susceptible refueling stations are infected and infected refueling stations are recovered. The process equations, using the Euler method, for the Kalman Filter are then set as: (where dt is taken to be 0.25 day)

$$S_k = S_{k-1} + (-\beta_{k-1} S_{k-1} I_{k-1})dt \quad \textit{Eq. 4}$$

$$I_k = I_{k-1} + (\beta_{k-1} S_{k-1} I_{k-1} - \gamma_{k-1} I_{k-1})dt \quad \textit{Eq. 5}$$

$$\beta_k = \beta_{k-1} \quad \textit{Eq. 6}$$

$$\gamma_k = \gamma_{k-1} \quad \textit{Eq. 7}$$

Where the time step dt is taken as 0.25 day. The output takes the form of:

$$y_{1,k} = S_k \quad \textit{Eq. 8}$$

$$y_{2,k} = I_k \quad \textit{Eq. 9}$$

The UKF (Unscented Kalman Filter) relies on the unscented transformation, which determines the statistics of a random variable through a non-linear transformation of an L-dimensional random variable x through a non-linear function y=f(x). It is assumed that the state vector x has a known mean $\bar{x}$ and initial covariance P_0. The general structure of the UKF is Kalman filter for linear systems consisting of a prediction step and a correction (or update step). The main goal of the UKF is to reduce the error in state estimation from a priori (k-1) value to a posteriori (k) value in each successive time, step dt, where k=1,2…, N and N is the dimension of entire time interval of 12 days divided in dt=0.25 time steps. The statistics of the function y can then be determined using the procedures listed in the UKF pseudo-code as shown in Table 1. In Step 1, we initialize the UKF by providing the initial values for state vector X_k when t=0 days (k=1), shown above. For our algorithm, we used the set the initial values of S_k and I_k similar to the data provided by Gasbuddy for Day 1. This is because the initial values of these states are well known ahead of the estimation process. Initial values for β and γ were set to zero as they are to be determined via the estimation process. The initial covariance, P_0 was set to the identity matrix of size n by n, where n=4, the dimension of the state vector X_k. The tunable parameters Q and R for the assumption of

initial noise in the estimation and update process, for w_k and v_k matrices, were set as identity matrices which were tuned later to reduce error. The tuned matrices for noise assumption are shown in Table 1. New P, In Step 2, the scaling factors were defined by assuming Gaussian distribution and weighing matrices W_m and W_c are computed. In Step 3, (2L+1) number of Sigma points (χ_{k-1}) are generated using the scaling factor, λ, to carry out the non-linear unscented transformation of each a priori (k-1) states in the state vector, X_{k-1}. The sigma points are then transformed into $\chi_{k|k-1}$ using the non-linear system equations shown in Eq 4,5,6 and 7 with added noise estimates, w_k, for every time step. In Step 4, the mean of predicted states, $\hat{X}_{k|k-1}$, is computed by summing up the product of all sigma points and their respective weighing matrix for each state in X_k. In Step 5, observations from the estimations are generated by computing $\Psi_{k|k-1}$, which are the sigma points corresponding to the states S_k and I_k for every time step (dt). Using $\Psi_{k|k-1,}$ the mean of the predicted output, $\hat{Y}_{k|k-1}$ is determined. In Step 6 and 7, the Kalman Gain is computed by determining the Covariance (P_k^{yy}) and cross covariance (P_k^{xy}). In Step 8, The mean of predicted state and observation and Gasbuddy data for each day pertaining to that shown in Eq 8 and 9 are then used in the update step to correct the posterior states to reduce estimation error. This process is then repeated until k=N. The states S_k and I_k are being updated in every time step, as are the states β and γ, defined by their relation to S_k and I_k in Eq 4 and 5. In this process we can estimate the transmission rate (β) and recovery rate (γ) for every time step from the data provided by Gasbuddy.

Table 1. Unscented-Kalman Filter estimation process

Step	Equation	Comment

1. Initialization	$X_0 = E[X_{k=1}], \hat{X}_0 = E(\hat{X}_{k=1})$, $P_0 = E\left[(X_{k=1} - \hat{X}_{k=1})(X_{k=1} - \hat{X}_{k=1})^T\right]$ $Q = w_1 = [[1e1\ 1e1\ 1e2\ 1e2] * I_{n\times n}$, $\quad R = [1e1\ 1e1] * I_{p\times p}$ $\left(P_k^{yy}\right)_{i=1} = R$ $\left(P_k^{xy}\right)_{i=1} = [0]_{L\times 2}$	k=1,2…, N. N= dimension of entire time interval divided in dt, time steps. i=1,2…, 2L+1. L= number of states in X_k.
2. Define Scaling Factor and compute weighing matrices	**Scaling factors** $\alpha = 1, \beta = 2$, $\kappa = 0$ $\lambda = \alpha^2(L + \kappa) - L, where\ L = size\ of\ X_k$ **Weighing Matrix** $W_m^1 = \frac{\lambda}{L+\lambda}$ $W_c^1 = \frac{\lambda}{L+\lambda} + (1 - \alpha^2 + \beta)$, $W_m^j = W_c^j = \frac{1}{[2(L+\lambda)]}\ for\ j = 2, \ldots, 2L + 1$	Assume Gaussian distribution
3. Generation of Sigma Points	$\sqrt{P_k} = Chol(P_k)$ $\chi_{k-1} = [X_{k-1} \quad X_{k-1} + \sqrt{(L+\lambda)P_{k-1}} \quad X_{k-1} - \sqrt{(L+\lambda)P_{k-1}}\ ]$ **Use the known nonlinear system equation f(x) in Eq 4,5,6 and 7 to transform the sigma points into:** $\chi_{k|k-1}^i = f\left(X_{k-1}^i\right) \quad for \quad i = 1,2, \ldots, 2L + 1$	Where Chol is a MATLAB function for the Cholesky Decomposition
4. Compute mean and covariance	$\hat{X}_{k|k-1} = \sum_{i=1}^{2L+1} W_m^i \chi_{k|k-1}^i$ $P_{k|k-1} = \sum_{i=1}^{2L+1} W_c^i \left(X_{k|k-1}^i - \hat{X}_{k|k-1}\right)\left(X_{k|k-1}^i - \hat{X}_{k|k-1}\right)^T$	$\hat{X}_{k|k-1}$ mean of predicted state
5. Generate Observations	$\psi_{k|k-1}^i = h\left(\chi_{k|k-1}^i\right)$ $\hat{Y}_{k|k-1} = \sum_{i=1}^{2L+1} W_m^i \psi_{k|k-1}^i$	$\hat{Y}_{k|k-1}$ mean of predicted output
6. Covariance and cross	$P_k^{yy} = \sum_{i=1}^{2L+1} W_c^i \left(\psi_{k|k-1}^i - \hat{Y}_{k|k-1}\right)\left(\psi_{k|k-1}^i - \hat{Y}_{k|k-1}\right)^T$ $P_k^{xy} = \sum_{i=1}^{2L+1} W_c^i \left(X_{k|k-1}^i - \hat{X}_{k|k-1}\right)\left(\psi_{k|k-1}^i - \hat{Y}_{k|k-1}\right)^T$	

covariance estimation		
7. Compute Variable Kalman Gain matrix	$K_k = P_k^{xy}\left(P_k^{yy}\right)^{-1}$	Required for updating state prediction and reducing estimation error.
8. Update covariance and state matrices	$X_k = \hat{X}_{k\|k-1} + K_k\left(y_k - \hat{Y}_{k\|k-1}\right)$ $where\ y_k\ the\ output\ matrix\ of\ data\ from\ Gasbuddy\ for\ each\ time\ step\ k.$ $P_k = P_{k\|k-1} - K_k P_k^{yy} K_k^T$	Step 2-8 is repeated for each time step k.

Refueling model using Optimal control

The Unscented-Kalman Filter provides estimate of the parameter β and γ, which are constant scalar values that can be used to develop a continuous time invariant dynamic model to characterize the fuel shortage as an infection. We now utilize this dynamic model to determine an optimal refueling strategy, which is modeled like a vaccination intervention, to control our epidemiological model of hurricane fuel shortage.

The SIR dynamics model is then augmented to include vaccination [25] as shown below:

$$\frac{dS}{dt} = -\beta S(t)I(t) - u_v S(t) \qquad \text{Eq 19.}$$

$$\frac{dI}{dt} = \beta S(t)I(t) - \gamma I(t)$$

In Eq 19, the new term u_v is the per capita rate of refueling. Keeping congruency with our model parameters, u_v is the rate at which susceptible gas stations are prevented from being emptied out every day by external intervention that provides extra amounts of gas supply.

This external intervention, seen in Figure 1(b) in the form of additional fuel supply can be provided by a governing agency or a private company. Before we proceed further, it is worth discussing the bounds on the control variable, u_v. This variable will be related to the refueling effort that is employed [25]. For example, the level of u_v that can be attained at any given time will, to some extent, depend on the infrastructure that is in place to overcome fuel shortage problems such as the amount of gasoline in reserve in proximity to the area in question, the availability of transport vehicles etc. With these bounds kept under consideration, we can assume that control resources are limited. This paper aims to determine an optimal strategy to refuel such that fuel shortage is kept at a favorable level throughout the interval being observed, subject to limited fuel resources.

Let r(t) denote the total number of refueled fuel stations that were susceptible to becoming empty (infected) at time, t. The actual values of S, I and r will depend on the specific choice of controls u_v. Then, if $r_{max} \geq 0$ is fixed, a control, u_v, will have to be determined for the augmented SIR model in Eq 19 that minimizes the cost function (J) shown in Equation 20. Similar approaches have been used for the vaccination analogue for infectious diseases [25].

$$J = \int_{t0}^{T} \beta S(t) I(t)\ dt \qquad \text{Eq 20}$$

subject to $S(t_0) = S_0, I(t_0) = I_0, T = \inf\{t \mid I(t) = I_{min}\}, u_v(t) \in \left[0, u_{v,max}\right]$ for all $t \in [0, T]$, and subject to the resource constraint

$$R = \int_{t_0}^{T} u_v S(t)\ dt\ \leq r_{max} \qquad \text{Eq 21}$$

where I_{min} is a threshold constant chosen to indicate the end of the gas station fuel shortage problem at some final time, T.

This optimal problem can be solved by applying Pontryagin's Maximum Principle (PMP). In its general sense, consider the following optimal control problem with isoperimetric constraints [24]:

$$\min J = \phi\big(T, x(T)\big) + \int_{t_0}^{T} L\,(t, x, u)\ dt$$

<u>*s.t.*</u>

$$\begin{cases} \dot{x} = f(t, x, u), x(t_0) = x_0, u \in\ U, \\ \int_{t_0}^{T} L_1(t, x, u)dt = 0\,, (Integral\ cost\ Function) \\ R = \int_{t_0}^{T} L_2(t, x, u)dt\ \leq r, (Resource\ Constraints) \\ \psi\big(T, x(T)\big) = 0 \\ \{\phi_x + [\phi_x]^T\vartheta - \lambda(T)\}^T|_T dx(T) + \{\phi_T + \vartheta^T\psi_T + H\}|_T dT = 0\ (Transversality\ Conditions) \end{cases} \qquad \text{Eq 21.}$$

where, $x \in \mathbb{R}^n$ is the state vector, $u \in \mathbb{R}^m$ is the control vector,

$\phi\ (terminal\ cost), L_1, L_2\ and\ \psi$ are vector functions. ϕ, L_1 are scalar functions. r is constant vector and U is an admissible control region, with continuous partial derivatives w.r.t all its arguments [24].

From the optimal control problem in Eq 21, the PMP states: if u*(t) is an optimal control with x*(t) being the optimal trajectory, there exists a non-trivial solution of vector functions

λ (costate functions) and nontrivial vector constant λ_1, λ_2 and ϑ such that the conditions discussed below are met:

$$\begin{cases} \dot{x} = f(t,x,u), \dot{\lambda} = -H_x^T(t,x,u,\lambda), \\ H(t,x,u^*,\lambda,\lambda_1,\lambda_2) \geq H(t,x,u,\lambda,\lambda_1,\lambda_2), \forall\ admissible\ u, \\ x(t_0) = x_0, \psi\big(T,x(T)\big) = 0, \\ H\big(T,x(T),u(T),\lambda(T),\lambda_1(T),\lambda_2(T)\big) = -[G_T^T(T,x(T),\vartheta)]^T, \\ \lambda(T) = G_{x(T)}^T(T,x(T),\vartheta), \\ \int_{t_0}^{T} L_1(t,x,u)dt = 0, \int_{t_0}^{T} L_2(t,x,u)dt \ \leq r, \\ \lambda_2^T\left(\int_{t_0}^{T} L_2(t,x,u)dt - z\right) = 0, \lambda_2 \geq 0, \end{cases} \quad \text{Eq 22}$$

where $H(t,x,u,\lambda,\lambda_1,\lambda_2) = L(t,x,u) + \lambda^T(t)f(t,x,u) + \lambda_1 L_1(t,x,u) + \lambda_2^T L_2(t,x,u)$ is the Hamiltonian, and $G\big(T,x(T)\big) = \phi\big(T,x(T)\big) + \vartheta^T\psi(T,x(T))$.

It will be useful tool to note that if the system described in Eq 21 is autonomous (time-invariant), the Hamiltonian, H, is constant such that [24]:

$$H(t,x,u,\lambda,\lambda_1,\lambda_2) = const, \forall t \in [t_0,T].$$

Optimal Refueling Strategy

The deterministic SIR model for refueling with limited resources can be modeled by the governing equations shown in Eq 19 with addition of the resource constraint derivative shown in Eq 23

$$\dot{r} = u_v S \quad \text{Eq 23}$$

If we construct this problem as a maximization problem, then Pontryagin's Maximum Principle (PMP) can be used to develop the relationship:

$$H(t) = -\lambda\beta SI - \lambda_S\beta SI - \lambda_S u_v S + \lambda_I\beta SI - \lambda_I\gamma I + \lambda_r u_v S \quad \text{Eq 24}$$

where the costate equations are satisfied as follows:

$$\dot{\lambda_S} = -(\lambda_I - \lambda - \lambda_S)\beta I - (\lambda_r - \lambda_S)u_v \quad \text{Eq 25}$$

$$\dot{\lambda_I} = -(\lambda_I - \lambda - \lambda_S)\beta I + \lambda_I\gamma \quad \text{Eq 26}$$

$$\dot{\lambda_z} = 0$$

For this problem, from Eq 21, the terminal cost and terminal constraint is 0. Hence, the transversality conditions can be reduced to:

$$\underline{\lambda}^T(T)d\underline{x}(T) + H(T)dT = 0 \quad \text{Eq 27}$$

where $dx(t) \neq 0$ since there are no terminal constraints on any of the states. dT= 0 as there is some fixed T. $\underline{\lambda}^T(T) = [\lambda(T), \lambda_S(T), \lambda_I(T), \lambda_z(T)]$, respectively.

Applying the PMP in Eq 22, we can postulate:

$$H(t, x, u^*, \lambda, \lambda_1, \lambda_2) \geq H(t, x, u, \lambda, \lambda_1, \lambda_2), \forall\ admissible\ u \quad \text{Eq 28}$$

$$-\lambda_S u_v^* S + \lambda_{z\backslash r} u_v^* S \geq -\lambda_S u_v S + \lambda_r u_v S$$

$$u_v^* S(\lambda_r - \lambda_S) \geq u_v S(\lambda_r - \lambda_S)$$

The optimal control then becomes bang-bang control [24] where the switching function is given by $(\lambda_r - \lambda_S = 0)$ and satisfies

$$u_v^* = \begin{cases} u_{v,max}, \lambda_r > \lambda_S \\ ?, \quad \lambda_r = \lambda_S \\ 0, \quad \lambda_r < \lambda_S \end{cases} \quad \text{Eq 29}$$

Following the development in Ref [24] show that that the optimal control is purely bang-bang, and there is no singular component or discontinuity. If $\lambda_r = \lambda_S$ on some interval *B* then $\dot{\lambda_S} = 0$ on *B*. Eq 25 then can be simplified to:

$$0 = -(\lambda_I - \lambda - \lambda_S)\beta I - (\lambda_r - \lambda_S)u_v, (\, let\, u_v = 0) \qquad \text{Eq 30}$$

$$\lambda_I = \lambda + \lambda_s$$

We can further postulate that $\dot{\lambda_I} = 0$ on *B*. Hence, by Eq 26 and Eq 30, it must follow that $\lambda_I = 0$. Therefore, $\lambda_S = -\lambda$ and then the only nonzero criteria for the variables on *B* is $(\lambda, \lambda_S, \lambda_I, \lambda_r) = (1, -1, 0, -1)$. Furthermore, by Eq 25 and Eq 26, once u_v^* becomes singular, it must remain singular throughout the whole interval *B*. Since $T \in B$, $(\lambda, \lambda_S, \lambda_I, \lambda_r) = (1, -1, 0, -1)$ has to satisfy the transversality condition that $\lambda_S(T) = 0$ as shown in Eq 27. We can further postulate, that since this boundary condition posed by the transversality condition is not met, the optimal control is purely bang-bang control. Now we examine the time at which the optimal control switches from 0 to $u_{v,max}$. Let the switch time be at t_s [24, 29]. Then the Hamiltonian, H, at switching time, t_s can be written as follows:

$$H(t_s) = -\dot{\lambda_I}(t_s)I(t_s) = -\dot{\lambda_S}(t_S)S(t_s) - \lambda_I(t_s)\gamma I(t_s) = 0 \qquad \text{Eq 31}$$

By substituting $\dot{\lambda_I}(t_s) = 0$ into Eq 26 gives

$$(\lambda_S(t_s) + \lambda)\beta S(t_s) = \lambda_I(t_s)(\beta S(t_s) - \gamma) \qquad \text{Eq 32}$$

Considering the relations in Eq 29 and Eq 31, the pure bang-bang optimal control is defined:

$$\lambda_I(t_s) > 0 \; when \; \dot{\lambda_S}(t_s) < 0 \rightarrow \left(0 \rightarrow u_{v,max}\right) \qquad \text{Eq 33}$$

$$\lambda_I(t_s) < 0 \; when \; \dot{\lambda_S}(t_s) > 0 \rightarrow \left(u_{v,max} \rightarrow 0\right)$$

$$\lambda_I(t_s) = 0 \; when \; \dot{\lambda_S}(t_s) = 0 \rightarrow (no \; switch \; occurs)$$

Since $\lambda_S(t_s) = \lambda_r = const., \lambda_S(t_s) + \lambda$ is either always positive, always negative or always zero. Suppose $\lambda_S(t_s) + \lambda = 0$. Then, by Eq 32, either $\lambda_I(t_s) = 0 \; or \; S(t_s) = \frac{\gamma}{\beta}$. By Eq 33, if $\lambda_I(t_s) = 0$, then no switching occurs. Hence, it can be postulated that if $S(t_s) = \frac{\gamma}{\beta}$ then the optimal control has only one switch and this switching occurs when I(t) is maximum, since S(t) is a monotonically decreasing function of time [24]. So, the possible control switches are:

$$u_v^* = \begin{cases} u_{v,max}, t \in [0, t_s) \\ 0, \quad t \in [t_s, T] \end{cases} \qquad \text{Eq 34}$$

we consider $\lambda_S(t_s) + \lambda > 0$. By using the relations derived in Eq 32 and Eq 33 we can postulate [12]:

$$(i) \; \lambda_I(t_s) > 0 \; and \; S(t_s) > \frac{\gamma}{\beta} \; \; or \qquad \text{Eq 35}$$

$$(ii) \; \lambda_I(t_s) < 0 \; and \; S(t_s) < \frac{\gamma}{\beta}$$

Thus, by tracking the value of S(t) we can develop an algorithm to switch the control and determine the switching time analytically. In this SIR model for fuel shortage, the switching time, t_s, refers to the time when one should supply extra fuel to the operating fuel stations (susceptible at time t), to keep them operational in order to optimally control the fuel shortage epidemic to favorable levels.

Results

Parameter Estimation

The Unscented Kalman Filter was implemented to estimate the state variables and parameters of epidemic dynamics based on measured empirical data from Gasbuddy. The empirical data allow for a quantitative comparison of the filter in estimating the states for the process equations shown in the methods section.

In Figure 2(a) the transmission rate per capita (β) and the recovery rate (γ) is shown, for Miami/Ft Lauderdale area, that were estimated by the UKF for each time step, dt. It is evident from Figure 2(a) that, due to the discontinuity and fluctuations of the empirical data provided by Gasbuddy, there is an inherent parameter variation observed in Figure 2(a). High standard deviation of the plots in Figure 2 (a) shows rate of change of transmission rate per capita (β) from day to day causing discontinuities in the model. The estimated β rate is almost 0.05 for the beginning of Day 2 compared to 0.0029 in Day 1, signaling a high demand for fuel causing an increase in the number of fuel stations. The γ rate shows a gradual increase as time goes on, showing that as the hurricane moves further north, more fuel stations become operational. In Figure 2 (b) we can see that estimated data for the continuous time invariant SIR model shows close resemblance to the real-life data provided by Gasbuddy.

As established in the Methods section; a constant parameter SIR dynamical system is used for the application of an optimal refueling strategy. In order to achieve that, the transmission rate per capita (β) and mean of all the recovery rates (γ) estimated by the UKF were chosen from Figure 2(a). These chosen parameters were used to compute the SIR data that have the best fit with the empirical data (using the Euler Method shown in Eq 4 and 5). This was done

by visual inspection and computing the root mean square (RMS) error for every transmission rate per capita (β) value, estimated by the UKF, for the Miami/Ft Lauderdale area. The transmission rate per capita (β) value with the least RMS error and best fit was chosen for the estimated data plot in Figure 2(b). Moreover, the constant recovery rate (γ) that was determined also reflected the mean infection period (1/γ) observed in the empirical data. Compared to the Miami/Fort Lauderdale area, the city of Orlando much lower values of transmission per capita (β) was observed for the city of Orlando, as shown in Figure 3(a). This is indicative of the fact that fuel shortages were much fewer in Orlando to compared to Miami/Fort Lauderdale area due Orlando's location being north of hurricane Irma's landfall. Other key factors that contributed to this phenomenon are Orlando's lower number of evacuees, fuel stations and traffic flow compared to Miami/Fort Lauderdale. Due to Miami/Fort Lauderdale's location being the southernmost in relation to the hurricane's location the mean recovery rate (γ) is lower compared to that estimated for Orlando.

The continuous time invariant model SIR data for the rest of the four cities were computed in a similar way tabulated in Table 2 and the estimated SIR data shown in Figure 4. The most noticeable difference was in the β and γ values, that were determined. The UKF estimation of β and γ values were unique to every city. The data computed for Jacksonville and Orlando were not able to reflect similar maximum number of empty fuel stations that was observed in the Gasbuddy data, but these were the data curves that had the least root mean square error. The estimated data for the Tampa/St Petersburg, Fort Myers/Naples and West Palm area shows a sufficient fit with the real-life data from Gasbuddy.

As it can be seen from Table 2 the recovery rate (γ) is approximately similar for all the cities affected by hurricane Irma. This concurs to the fact that a similar mean infection period for

fuel shortage is observed by all the cities during the evacuation period. This is reflected in the empirical data, as it can be seen in Figure 2, the infection (i.e. fuel shortage) stops around the same time as the number of infected fuel stations start reducing corresponding to no more infection being present. It is also seen that during that same time the estimated data show a change in curvature corresponding to an increased rate of reduction in infected refueling stations.

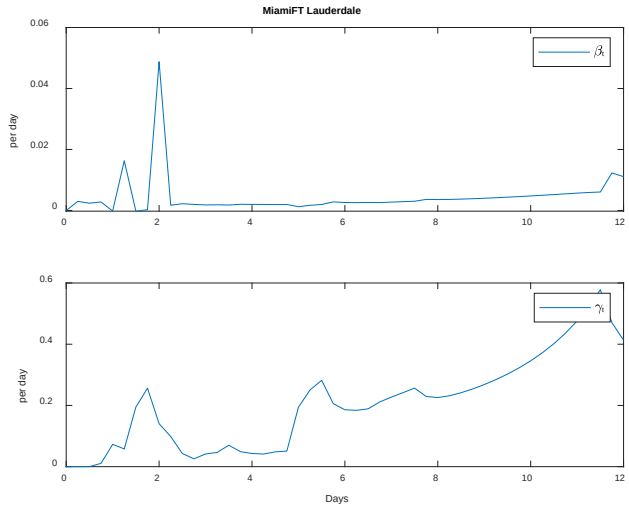

Figure 2(a). β and γ rates estimated from data provided by Gasbuddy for each time interval dt over the entire time interval for Miami/Fort Lauderdale

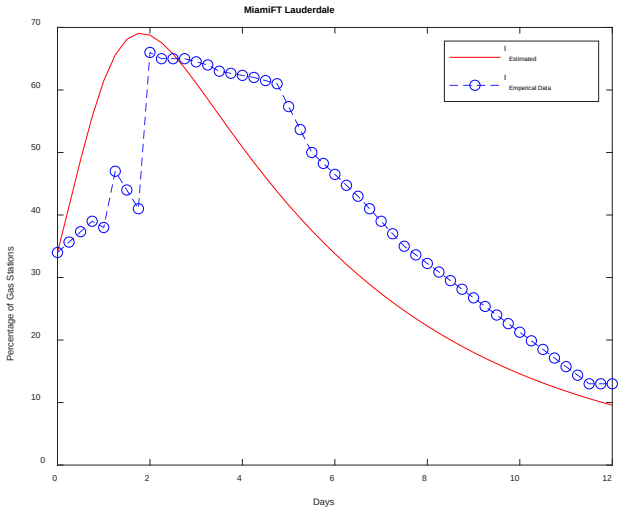

Figure 2(b). Continuous time Invariant data computed from estimated constant parameters compared to the real-life crowdsourced data gathered by Gasbuddy for Miami/Fort Lauderdale area for Percentage of empty fuel stations.

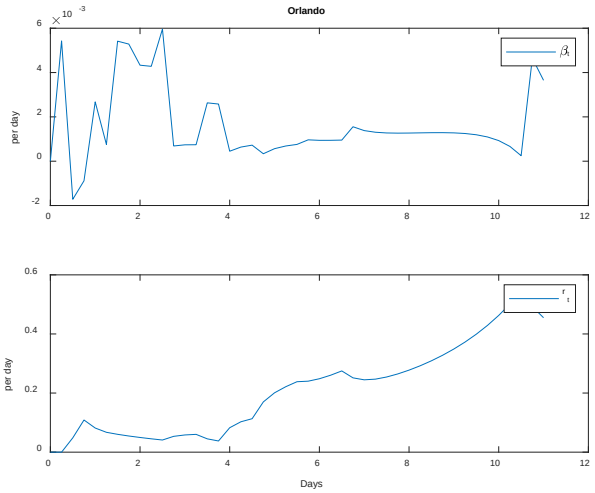

Figure 3(a). β and γ rates estimated from data provided by Gasbuddy for each time interval dt over the entire time interval for Orlando.

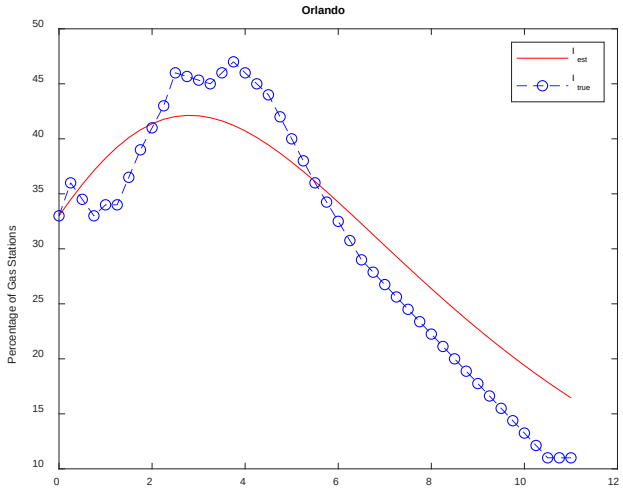

Figure 3(b). Continuous time Invariant data computed from estimated constant parameters compared to the real-life crowdsourced data gathered by Gasbuddy for Orlando city for Percentage of empty fuel stations.

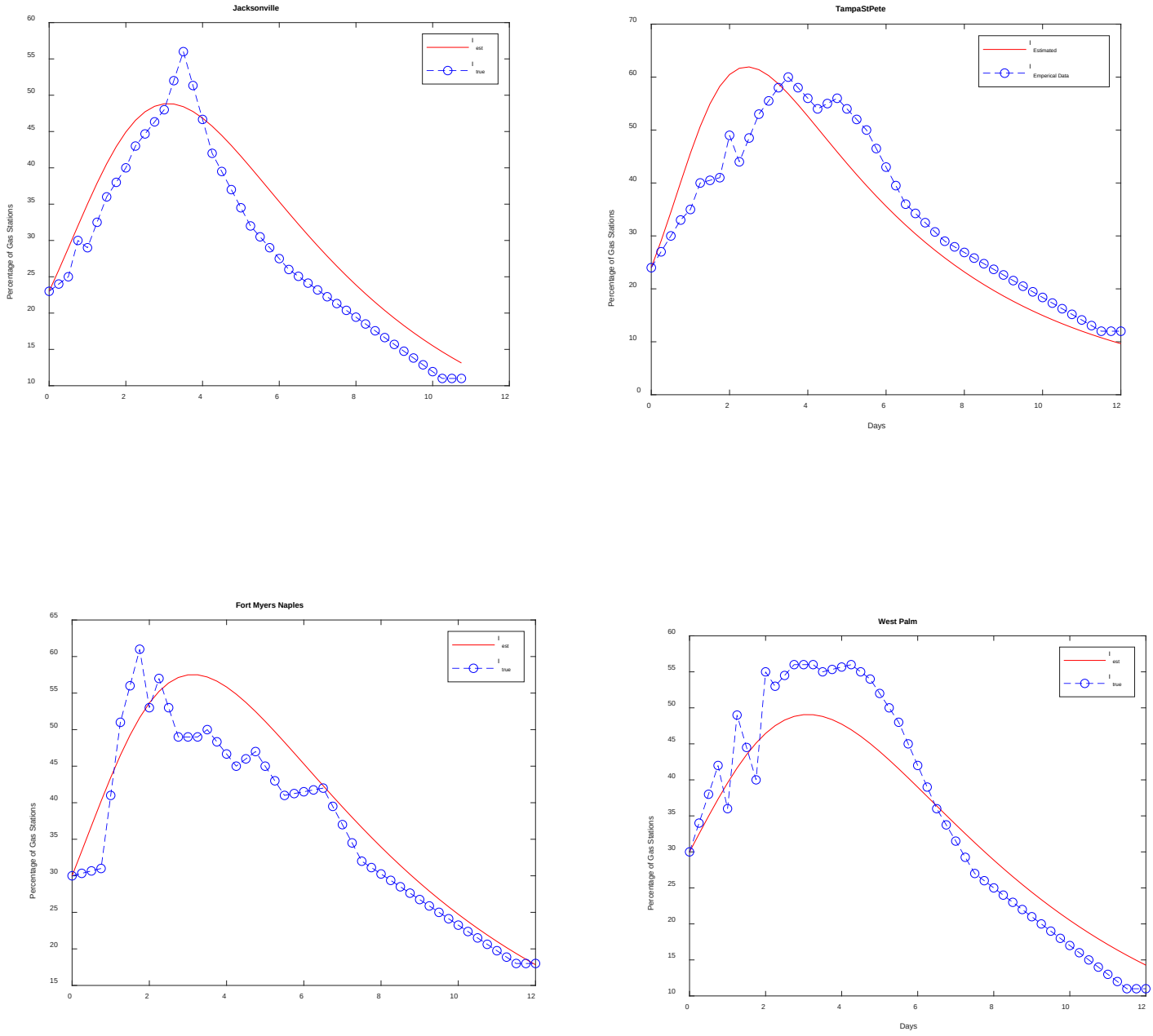

Figure 4. Continuous time Invariant data for percentage of empty fuel stations computed from estimated constant parameters compared to the real-life crowdsourced data gathered by Gasbuddy for Jacksonville, Tampa/St Petersburg Area, Fort Myers/ Naples Area and West Palm

The estimated β and γ rates are provided in Table 2.

Table 2. β, γ and R_0 parameters shown along with various geographical and demographical data of the city being affected.

City/Area	γ	β	R_0	City Area (mi^2)	No. of cars in area	Distance from South
Jacksonville	0.237	0.00969	2.86	874.6	830617	399.23
Orlando	0.210	0.00579	1.93	113.8	270831	276.00
Tampa/St Pete	0.217	0.01389	4.49	312.9	589384	238.00
West Palm Beach	0.200	0.00762	2.67	57.7	89030.00	184.00
Fort Myers-Naples	0.169	0.00887	3.67	65.4	61319	143.00
Miami/Fort Lauderdale	0.206	0.01629	5.54	6137.0	2663214	129.67

Optimal Control

The next step was to run an optimal refueling control algorithm that was derived in the methods section for the SIR deterministic model in Eq 19. The transmission rate per capita (β) and recovery rate (γ) were determined from the Gasbuddy Data using the UKF. Using the theorem used in the Method section, results for optimal control strategy were computed for all 6 cities for per capita rate of refueling ($u_{v,max}$) ranging from 0 to 0.75. Eq 19 and 35 were used to develop the continuous time data shown in Figure 5 (a), (b) and (c).

In the figures for optimal refueling strategy, we see, by varying the resource constraint, we vary the control variable per capita rate of refueling ($u_{v,max}$) to such an extent where the fuel shortage problem can be brought down to levels that are lower than the situation where there was no intervention. We believe that the optimal control strategy presents a solution where extra intervention can be provided and ended before the hurricane makes landfall, thus transporting fuel more safely to areas of high levels of fuel shortage.

The per capita rate of refueling ($u_{v,max}$) corresponds to the fraction of susceptible fuel stations, S(t), that will be provided with extra refueling scheme at a given time. Figure 5 (a), (b), (c) also shows the application of the refueling strategy by varying the resource constraint

(r_{max}) for the Miami/Fort Lauderdale area. Figure 5(a) shows the percentage of fuel station of the total remains operational per day. In Figure 5 (a), the baseline is the curve corresponding to u_v=0. When there is no refueling strategy being applied, the continuous time invariant SIR dynamics takes the form of the model characterized by Eq 1 and 2. The baseline corresponds to the data generated by using the UKF estimation process, and is the continuous time invariant representation of the data provided by Gasbuddy on empty fuel stations during hurricane Irma. Application of refueling strategy is indicated when $u_v > 0$. The different labeled plots represent the operational fuel stations when different per capita rate of refueling ($u_{v,max}$) is applied as an extra intervention to optimally control the fuel shortage problem. There is a total of 1,369 fuel stations in this area [31]. At a time t=1 day, in Figure 5 (a), for the plot representing the operational fuel station, S(t), at per capita rate of refueling ($u_{v,max}$) equal to 0.1, a total of (0.1*S(t=1)*1,369*15,000 gl) 534,115 gallons of fuel will have to supplied to be able to control the fuel shortage problem. The amount of extra fuel required for refueling strategy changes every time step as the number of operational fuel stations, S(t), changes per day. The application of the strategy helps reduce the number of empty fuel stations, I(t), per day as seen in Figure 5 (b). In Figure 5 (c), the application time and switching time of the optimal refueling strategy are demonstrated. Here the per capita rate of refueling ($u_{v,max}$) is applied from the beginning of the observed time window (12 days) and then switched to zero at the time designated by the condition shown in Eq 35. It is noteworthy that the application of the optimal refueling strategy can be done before the hurricane landfall occurs (in this case hurricane Irma makes landfall at Day 4 [26]) and the fuel shortage problem can still be controlled to favorable levels.

Figure 5 (b) also shows that for the area of Miami/Fort Lauderdale, the percentage of empty fuel stations can be reduced as hurricane evacuation is in effect. In this case the maximum percentage of empty fuel stations was reduced to 65%, compared to the base value of 70% with u_v=0.1. It was also observed that with the control variable ($u_{v,max}$), the maximum number of ineffective/empty fuel stations shifted earlier and is also lower. This means the worst possible scenario of a huge number of empty fuel stations happens earlier in the timeline considered compared to the baseline value. It is also evident the more u_v is provided at a given time the more efficiently and quickly we can control the spread of fuel shortage in any given area. But as the per capita rate of refueling ($u_{v,max}$) is increased over 0.5, the change in S(t) and I(t) gradually lessens. This is indicative of the fact that limited fuel injection is more effective when resources are scarce so resources can be distributed according to city/area concerned.

Fuel shortage in areas with higher number of fuel stations and concentrated traffic flow can be controlled using a lower per capita rate of refueling and vice versa. In the case of the city of Orlando, as shown in Figure 6 (a) and (b), the total number of fuel stations is 810. At time t=1 day, in Figure 6 (a), for the plot representing the operational fuel station, S(t), at per capita rate of refueling ($u_{v,max}$) equal to 0.1, a total of (0.1*S(t=1)*810*15,000 gl) 455,625 gallons of fuel will have to supplied to be able to control the fuel shortage problem which is less than Miami/Fort Lauderdale area seen in Figure 5 (a). This is because the continuous time invariant SIR model for the city of Orlando has lower transmission per capita rate and recovery rate. Due to that, the maximum ineffectives/empty fuel stations are different, and so are effect of the application of optimal refueling strategy. Miami/Fort Lauderdale area reportedly experienced higher rates of fuel shortage [16] compared to Orlando area.

Therefore, the reduction in maximum infectives in Figure 6 (b) is less than Figure 5 (b). Meanwhile the occurrence of maximum infectives in Orlando city is seen to happen much earlier than the baseline model when optimal refueling strategy is applied (per capita rate of refueling, $u_v > 0$).

We believe the optimal refueling strategy provides an effective solution to providing fuel to fuel shortage areas in a certain time interval that optimizes fuel delivery to help mitigate fuel shortage problems before the hurricane makes landfall in the concerned areas. Our strategy can also help develop policies to ensure minimal blockages in fuel supply as evacuation is in full effect leading up to the hurricane making landfall.

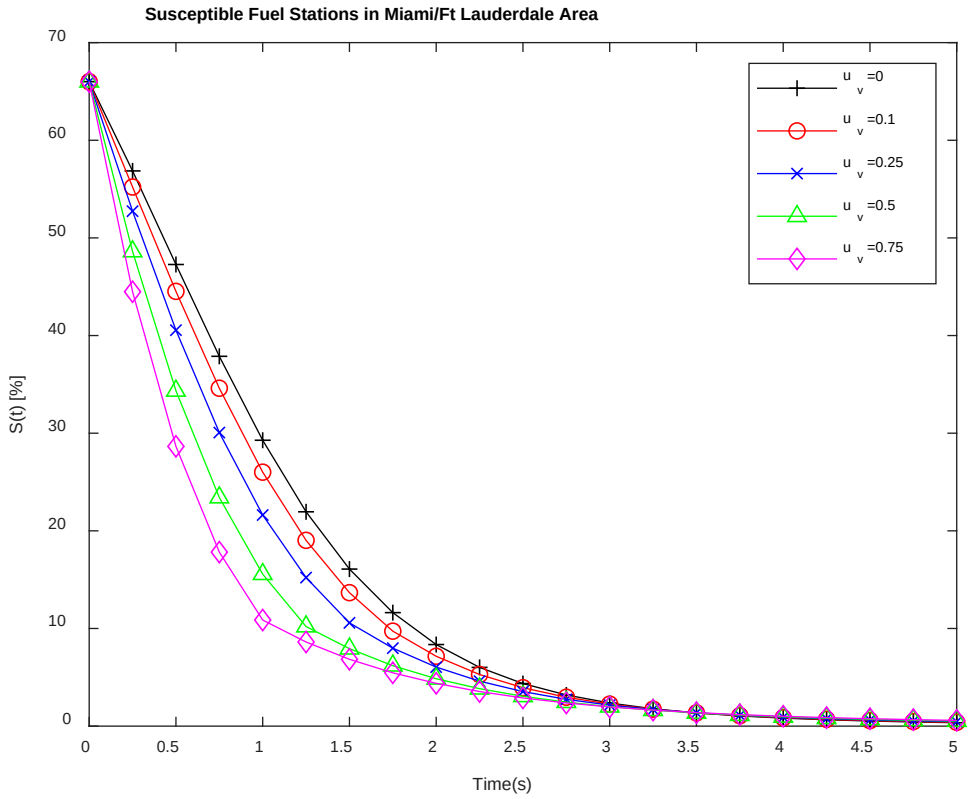

Figure 5(a). Susceptible/Operating Fuel Stations per day in Miami/Fort Lauderdale during Hurricane Irma

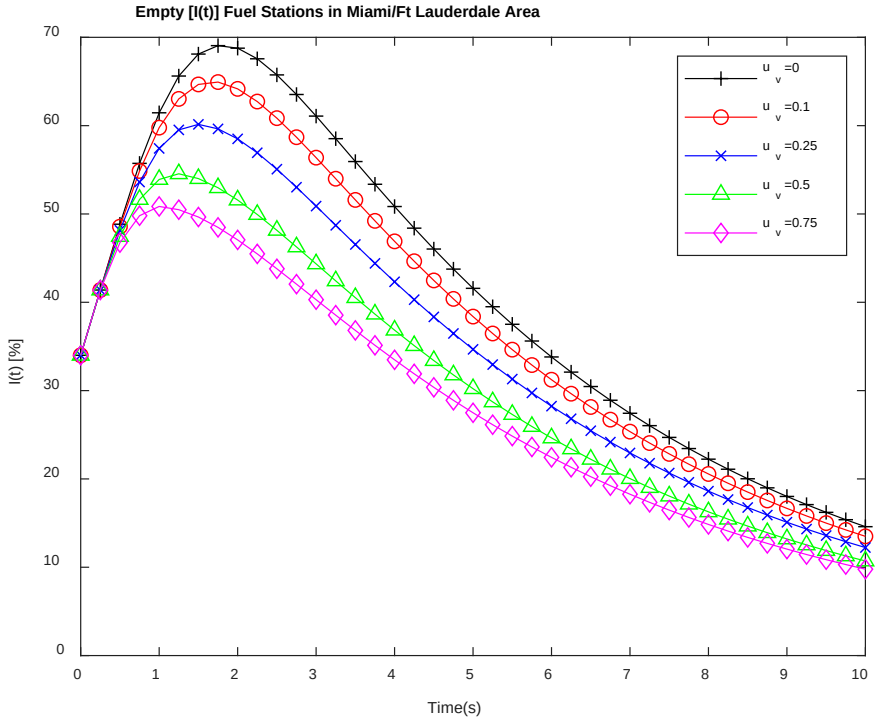

Figure 5(b) Infected/Empty Fuel Stations per day in Miami/Fort Lauderdale during Hurricane Irma

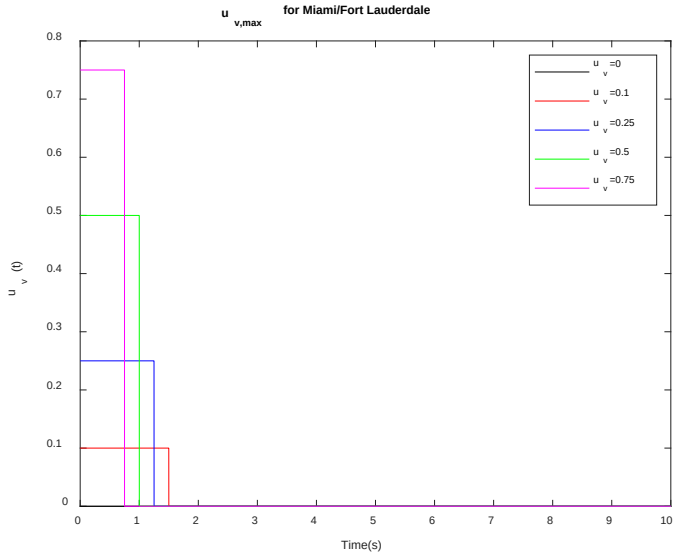

Figure 5 (c). Optimal refueling strategy for Miami/Fort Lauderdale area with varied resource constraint r_{max}, that result in varied u_v and switching time, t_s, for when refueling strategy can be ended.

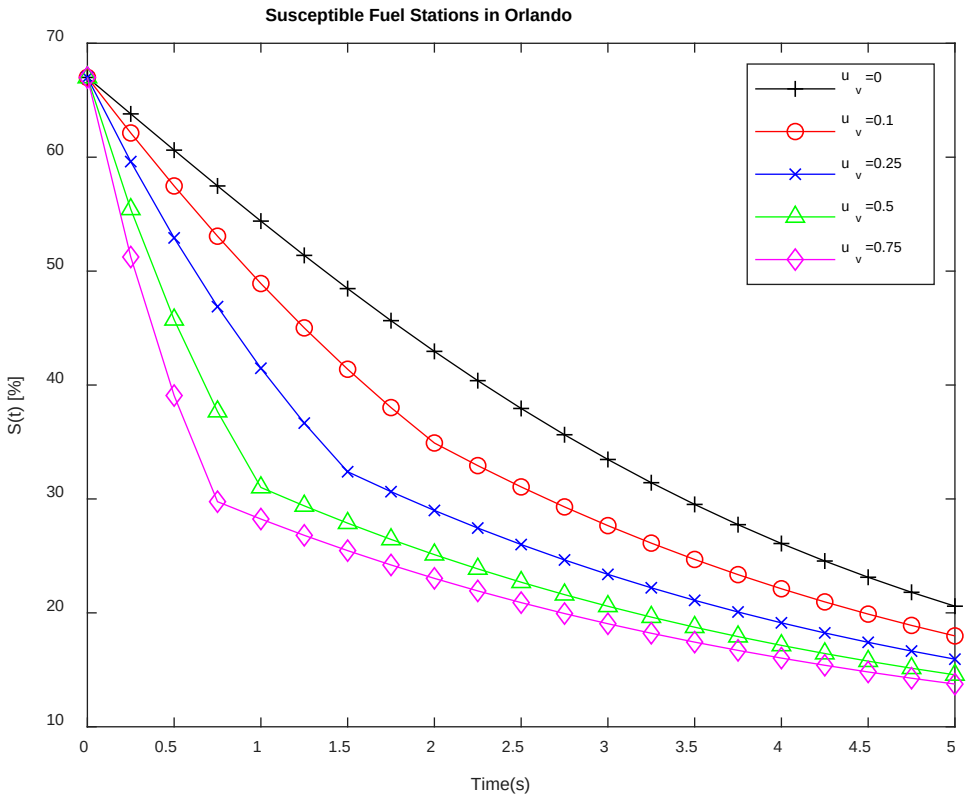

Figure 6(a). Susceptible/Operating Fuel Stations per day in Orlando during Hurricane Irma

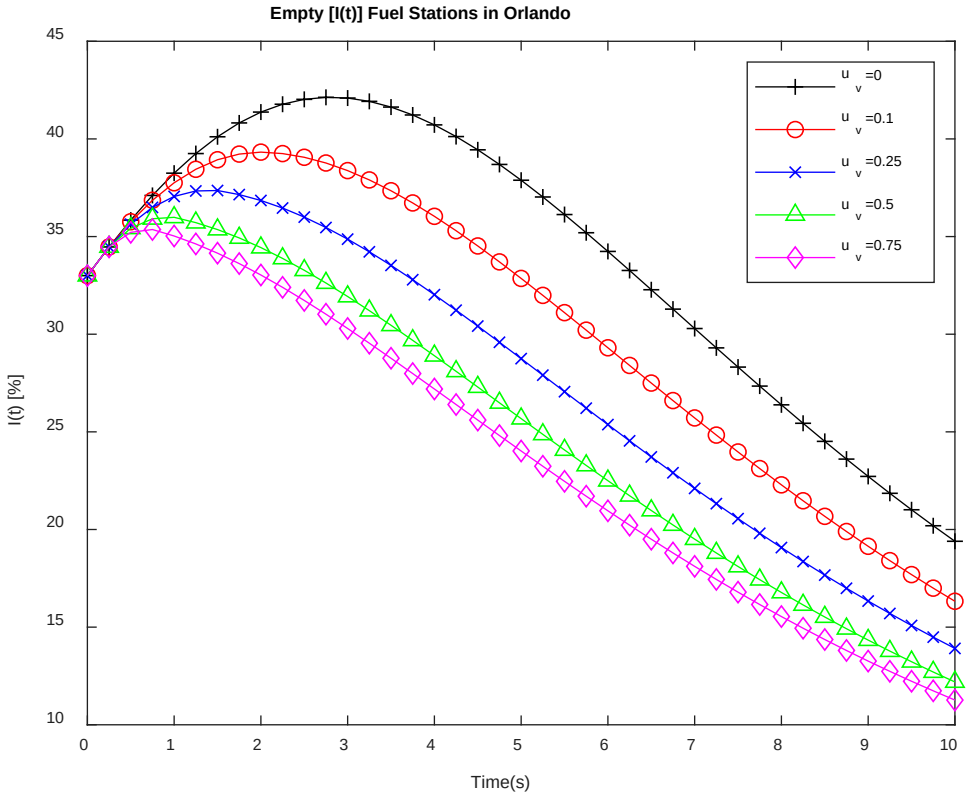

Figure 6(b) Infected/Empty Fuel Stations per day in Orlando during Hurricane Irma

A similar trend can be seen with the four other cities/areas as shown in Figure 7,8,9 and10. With higher u_v, the rate at which empty fuel station become operational again is increased. We can use this same approach for future hurricanes where we can use the UKF algorithm to estimate the transmission rate per capita and recovery rate from real life data in real time. By varying the severity of the "infection", which can be done by varying the R_0 value we can make parametrized predictions of the fuel shortage scenario ahead of time. We can then use the optimal refueling strategy to determine the best scenario for overcoming the fuel shortage problem in a specific city.

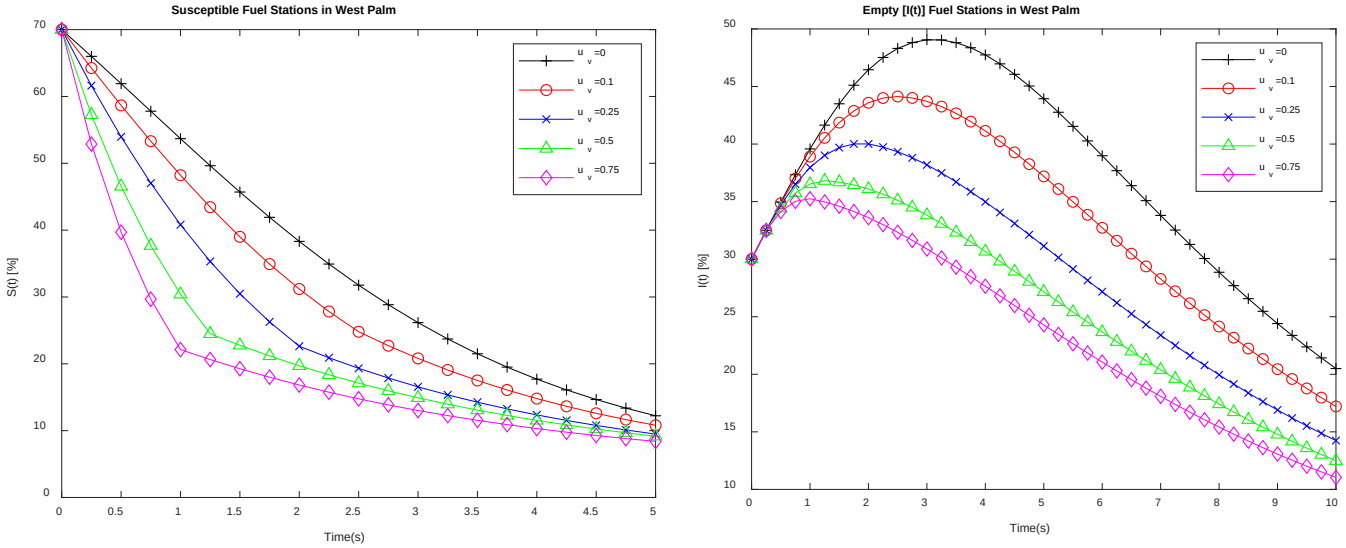

Figure 7. Susceptible/Operational Fuel Stations and Infected/Empty Fuel Stations in Fort Myers/ Naples

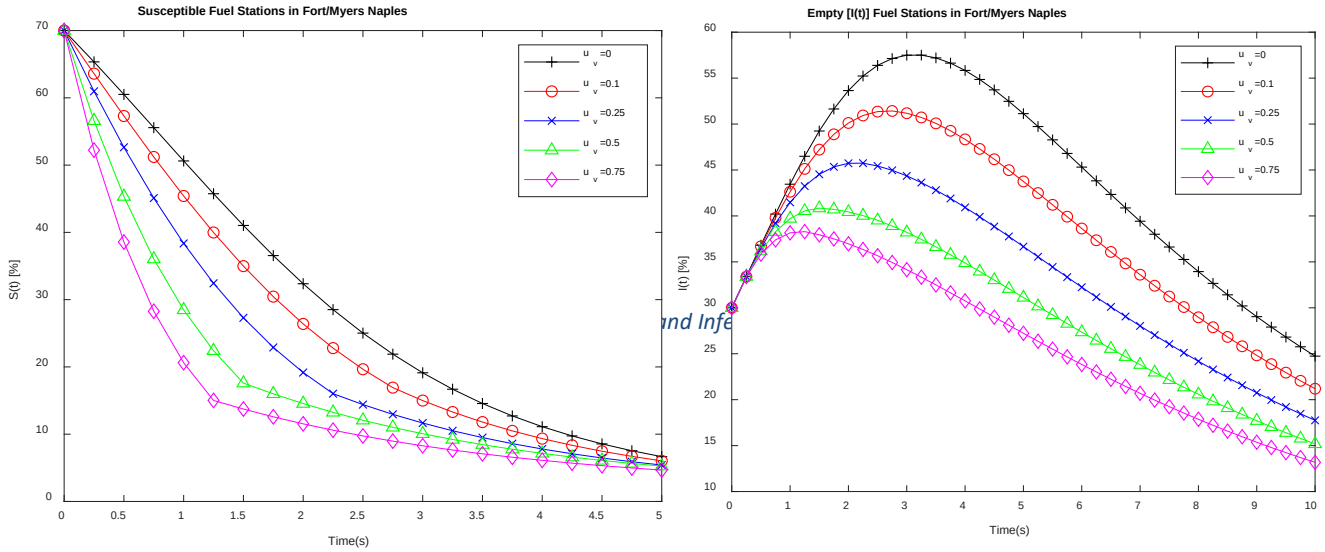

Figure 8. Susceptible/Operational Fuel Stations and Infected/Empty Fuel Stations in Fort Myers/ Naples

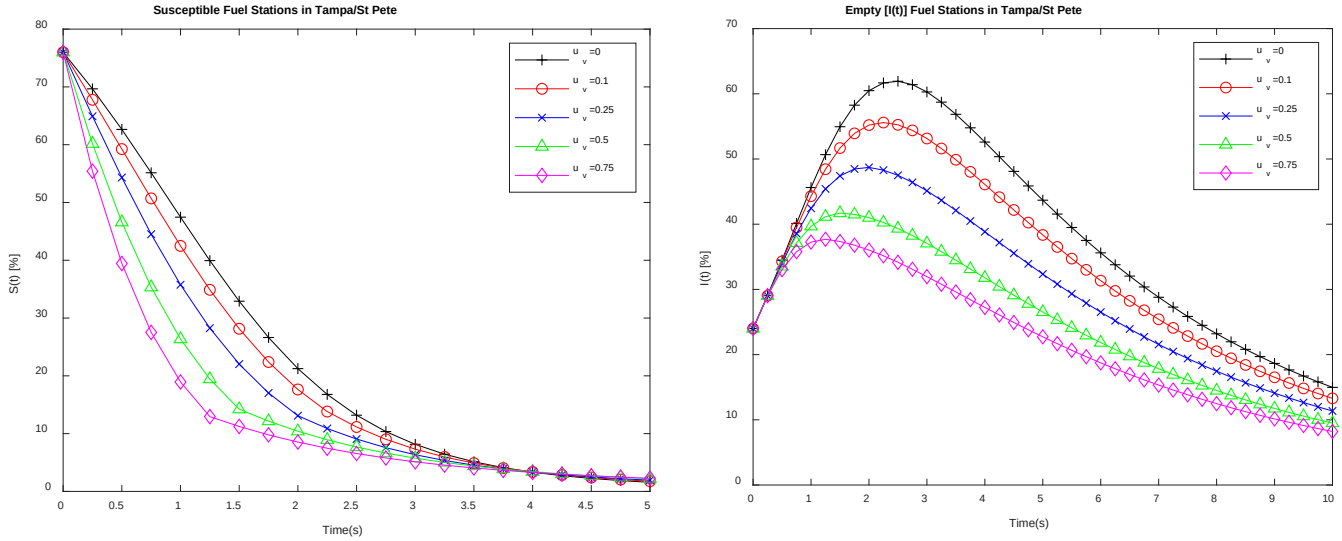

Figure 9. Susceptible/Operational Fuel Stations and Infected/Empty Fuel Stations in Tampa/ St. Petersburg Area

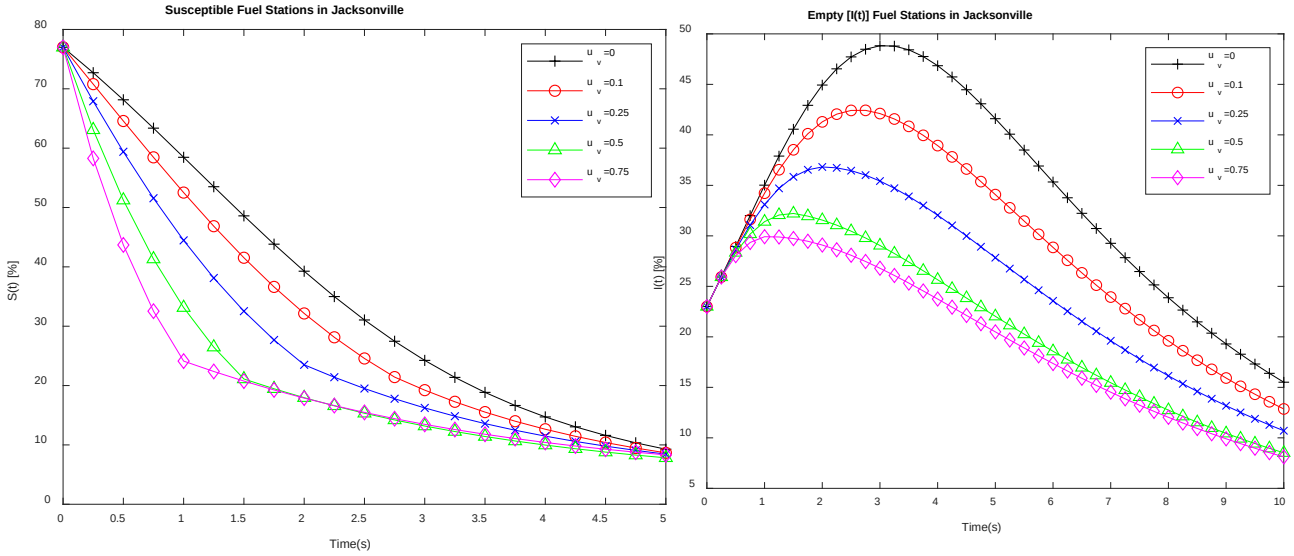

Figure 10. Susceptible/Operational Fuel Stations and Infected/Empty Fuel Stations in Jacksonville

Discussion

In this study, we used the Unscented Kalman Filter to estimate SIR dynamics parameters to develop an optimal refueling strategy for fuel shortage during a hurricane situation. Use of different Kalman Filter algorithms such as the Extended Kalman Filter (EKF) and Ensemble Kalman Filter (EnKF), in the field of engineering and epidemiology, is not uncommon. Sabet et al, demonstrates the use of EKF and UKF for an analytical approach to estimating the hydrodynamic parameters of an autonomous underwater vehicle (AUV) by providing persistent excitation of the vehicle in an underwater vehicle and using sensor data to update the prediction estimate [31]. A Recent study by Zhang also implemented the Kalman filter to predict the influenza trend in short terms [21]. This study makes use of the EKF, UKF and EnKF to provide quantitative comparison between synthetically produced SIR data (using filtering methods) with real life data from CDC and crowdsourced data from Twitter messages and Wikipedia access logs.

We believe our study is the first of a type that combines the use of Kalman filter techniques and optimal control strategy to provide solutions to a socio-economical problem that is modelled as a contagion. We used the UKF to estimate constant epidemiological parameters that enabled us to produce synthetic SIR data that closely resembled the real-life fuel shortage data provided by Gasbuddy. This approach enabled us to compare transmission rate per capita (β) and recovery rate (γ) for different cities/areas in Florida during the evacuation period of hurricane Irma as shown in Table 1.

The optimal refueling strategy demonstrated the use of an extra external refueling ($u_{v,max}$) to control fuel shortage and bring percentage of empty fuel stations to reduced levels. With the increase in per capita refueling rate ($u_{v,max}$), the law of diminishing returns starts to take

effect. One of the primary objectives of the optimal refueling strategy was to reduce the maximum percentage of empty fuel stations, I(t), during the evacuation time interval. In Figure 11, it can be seen that as $u_{v,max}$ is increased from 0 to 1, the change in maximum percentage of empty fuel stations, I(t), reduces. It is evident that there is an exponential relationship between $u_{v,max}$ and Max I(t). However, the change of maximum I(t) is observed to be more in areas with higher rate of fuel shortage, i.e. high transmission rate per capita (β). As seen in Figure 11, for the Miami/Fort Lauderdale area, with β=0.016/day there is a gradual reduction in maximum I(t) as $u_{v,max}$ is increased. In the case of Orlando city, with β=0.006/day, the maximum I(t) tends to reach an asymptote. Specifically after $u_{v,max}$=0.5, the plot of maximum I(t) for Orlando city shows minimal change. From this result, we can determine the refueling rate per capita ($u_{v,max}$) that is suitable for areas experiencing fuel shortage during hurricane evacuation based on the fuel distribution policy that the governing agency has chosen to adopt.

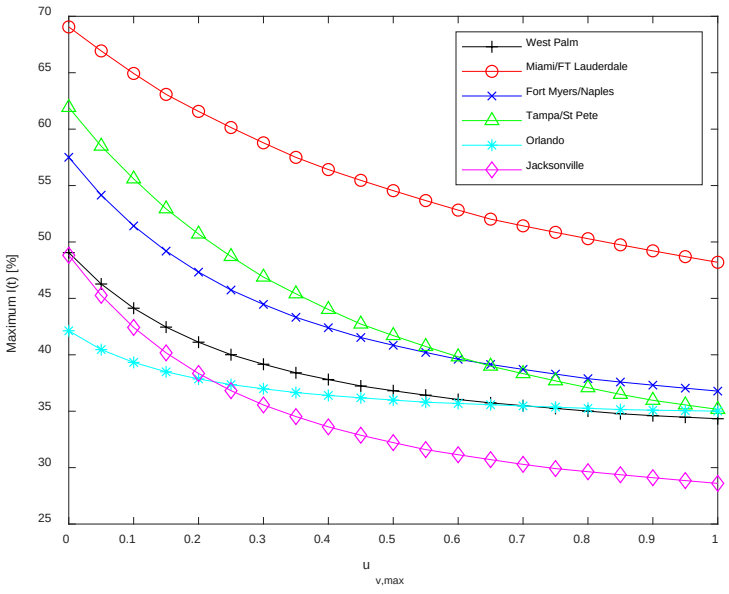

Figure 11. Maximum number of empty fuel stations, I(t), for $u_{v,max}$ ranging from 0 to 1.

To determine the best $u_{v,max}$ for a city/area, we performed bilinear interpolation. As it can be seen in Figure 12(a) and (b), using linear regression, 2 lines of best fit were computed for both Miami/Ft Lauderdale area and Orlando Area. The intersection of these lines helped us determine the best $u_{v,max}$ for that particular city/area. In the case of Miami/Fort Lauderdale area the best refueling per capita rate is 0.45, while for Orlando it is 0.25.

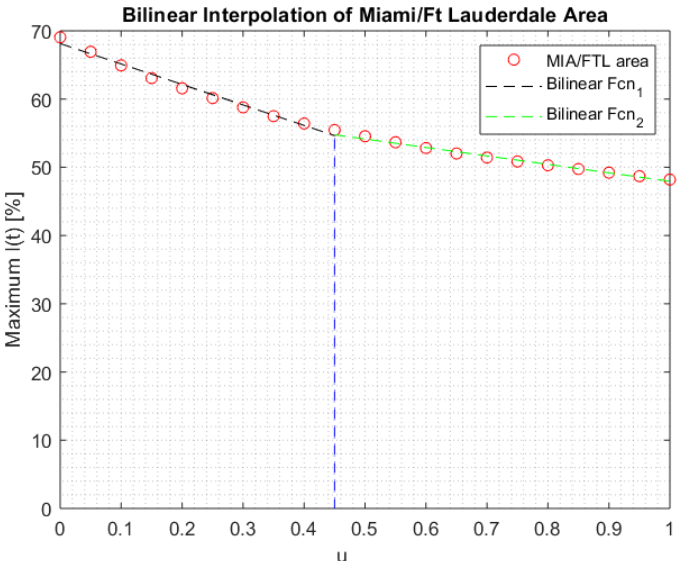

Figure 12 (a). Bilinear Interpolation of Miami/Ft Lauderdale Area to determine best u_v

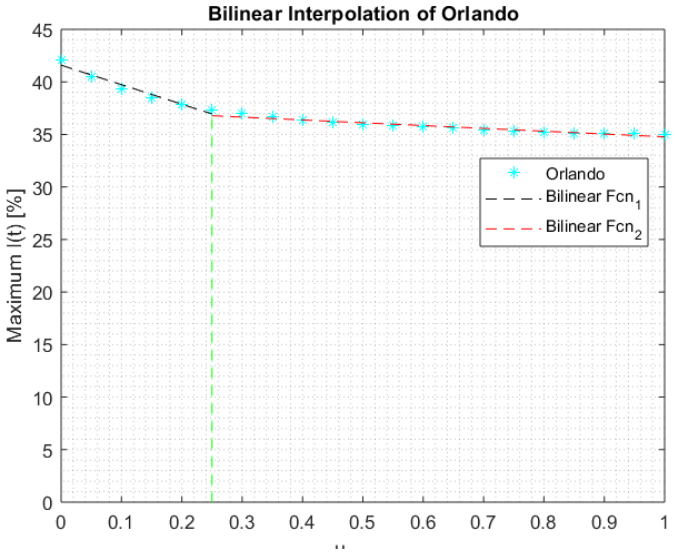

Figure 12(b). Bilinear Interpolation of Miami/Ft Lauderdale Area to determine best u_v

Conclusions

In this study, we used the data crowdsourced by Gasbuddy to model the fuel shortage experienced during hurricane Irma as a contagion. The contagion dynamics were based on first order differential equations based on SIR model. We used an Unscented Kalman Filter to compute the transmission rate per capita (β) and recovery rate (γ) from initial set of data points on number empty fuel stations provided by Gasbuddy or any other crowdsourced data provider for six different cities/areas. The β and γ rates that were computed were then used to

develop a smooth continuous curve that fit the real-life data. The basic reproduction number (R_0) was then computed for each and every city/area to correlate that to demographical data of the concerned areas. It was found that Miami/Ft Lauderdale area experienced the highest rate of fuel shortage with an R_0 value of 5.54. Whereas places such as Orlando, which are more inland and less through traffic, experienced reduced rate of fuel shortage with an R_0 value of 1.93. With the mechanistic data computed using the UKF estimated β and γ rates, an optimal refueling strategy was developed using Bang-Bang Control theory. The optimal control strategy provided us with a useful insight into the control of a contagion using vaccination rates. In this study we modeled the vaccination component of the SIR model as a per capita rate of refueling ($u_{v,max}$). The $u_{v,max}$ is an outside intervention, where extra amount fuel is provided by a governing agency that help mitigate and control fuel shortage to optimal levels with fuel resource constraints. With varying rate of vaccination, we are able to show, how the maximum number of empty fuel station changes and reach an asymptote due to the law of diminishing return. By using bilinear interpolation, we were able to develop a method by which we were able to ascertain that best per capita rate of refueling ($u_{v,max}$) for a given city/area. We determined that for Miami/Ft Lauderdale area the best $u_{v,max}$ is 0.45. While for Orlando City, the best $u_{v,max}$ is 0.26, respectively.

CHAPTER 2. AGENT BASED SIMULATION OF FUEL ALLOCATION AT AN INTERSECTION

Simulation Procedure

This model aims at testing the refueling capabilities of gas stations along the highway during the hurricane season in Florida State. Two data groups are used to compare in the experiment. Both models were run for 50 replications through 22 hours. Based on FDOT traffic data, we are supposed to obtain 12,000 vehicles per hour travelling along the highway. However, due to the limitation of the Anylogic Software in the speed of producing car, we tested a total number of 39,000 cars been produced.

Shown in Figure 13, the base group is that every single car coming to the gas station can fully fill their tanks. It is assumed that there are 6 gas stations along the highway for experiment and the capacity of each gas station is 10 cars at the same time. Each gas station has 20,000 gallons fuel in total. Only the cars have less than 5 gallons fuel will go into the gas station and fuel their cars, which accounts for 70% of cars in the experiment need to be fueled. When the first gas station is fully occupied or no fuel anymore, the cars needing to be fueled will automatically go into the next gas station. Similarly, if the second gas station is busy or empty, they will automatically go into the third one. However, the experimental group has the requirement that each car coming to fuel can only add 5 gallons fuel. Through the experiment, we can see the differences in figures and tables regarding how different two data groups perform.

Baseline Statistics

The baseline model is actually from the real operations of gas stations along the I-95 interstate within Volusia County during hurricane evacuation. Every single car coming to the gas station can fully fill their tanks. The baseline model shows a mean of 28.47% in terms of

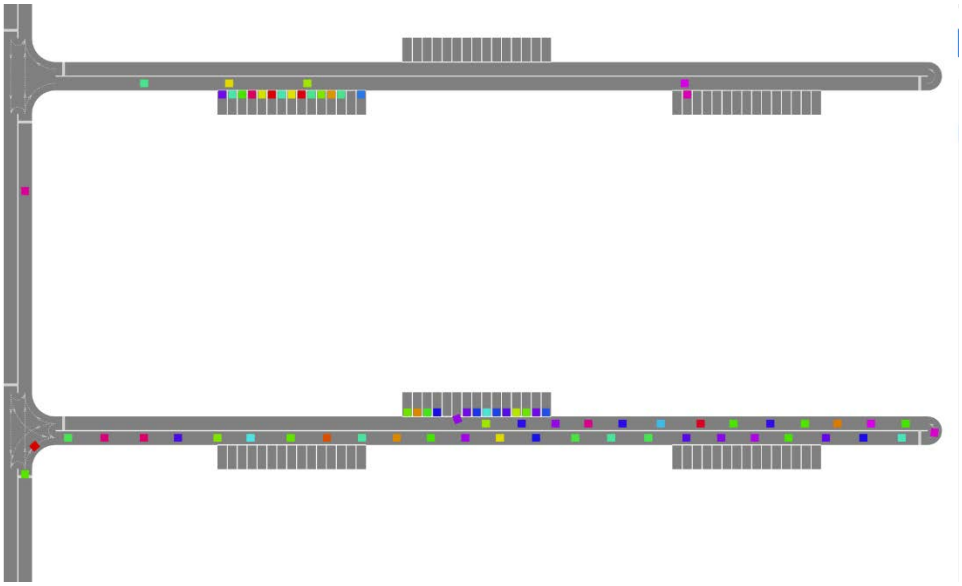

Figure 13. Fuel Station Schematic of agent based simulation.

percentage of vehicles successfully refueled. As stated previously that we set 30% of cars don't need to be fueled, which is more realistic, this caused the mean of percentage of vehicles successfully refueled being lower.

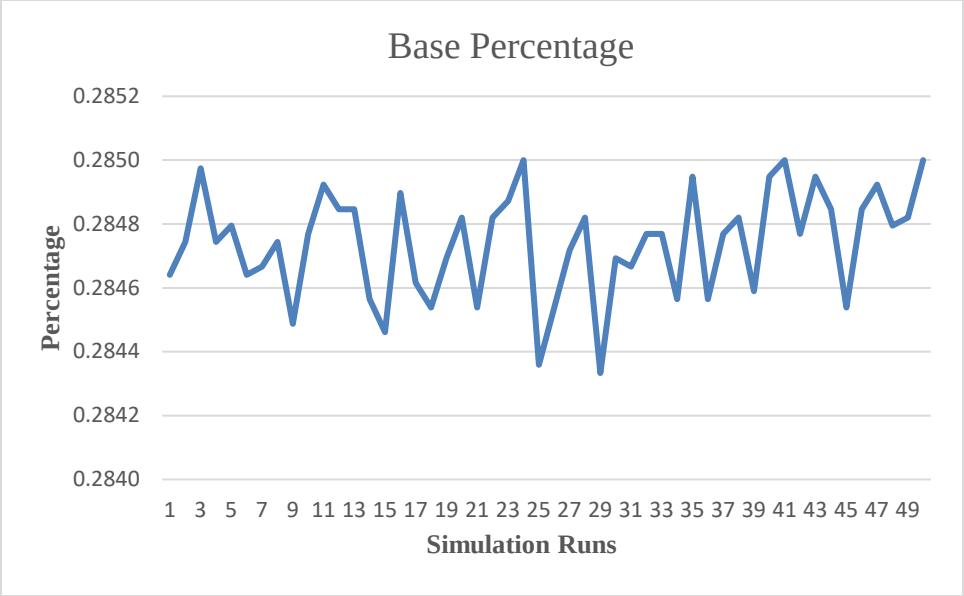

Figure 14. Baseline vehicles refueled successfully percentage.

Following figure represents the vehicle count of cars not being successfully fueled in each simulation run. The reason of these cars not being successfully fueled is that if the gas station is fully occupied or no fuel anymore, the car will automatically turn into the next gas station until the last one. However, if the last gas station has no fuel as well, this car will be regarded as not successfully fueled. According to the data, the speed of producing car is that every two seconds produces one car. As a result, an average of 16,217.93 vehicles ran out of gas within the simulation model and not being successfully refueled. The data acquired is graphically presented in Figure 2:

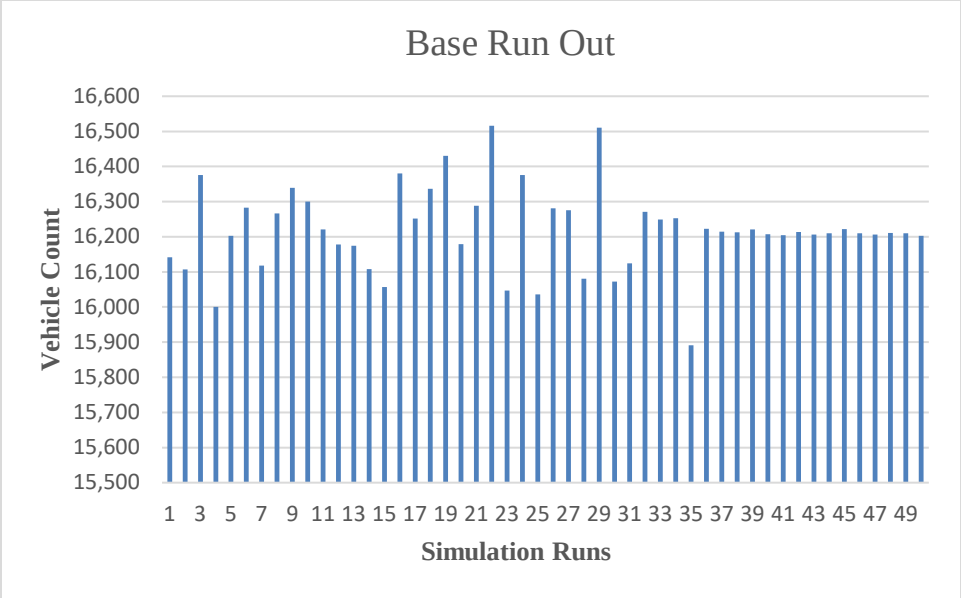

Figure 15. Baseline vehicles running out of gas.

Experimental Statistics

The experimental model was conducted based on the settings of the base one. The only difference is that the experimental model has a 5 gallons limitation of refuel amount. As a result of the restriction, the percentage of vehicles that have been refueled successfully has increased. As the Figure 3 shows, the control of the amount of gas had changed the results a lot. Due to the limitations of fuel quantity, the percentage of successfully fueled vehicles has jumped from 28% to 62% comparing to the baseline model.

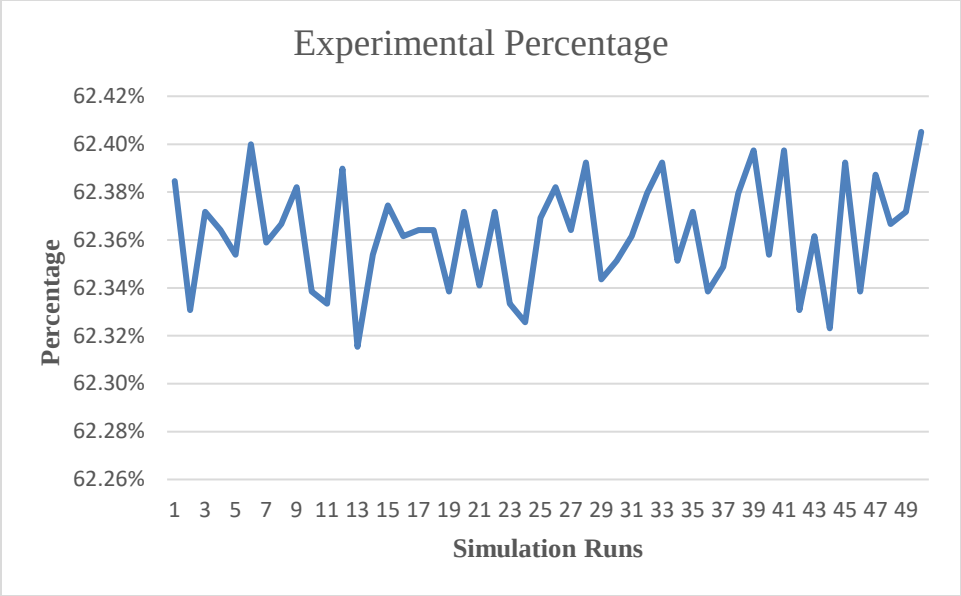

Figure 16. Experimental vehicles refueled successfully percentage.

Because of the control measure on refueling of vehicles, the amount of vehicles that ran out of fuel has decreased obviously. As the Figure 4 indicates, comparing to the baseline model, the amount of vehicles that ran out of gas has decreased from 16,218 to 3,016. The decrease mean that more vehicles has escaped from the destiny of running out of fuel. Meanwhile, less traffic jam will happen along the highway, which can make the evacuation of hurricane season more smoothly.

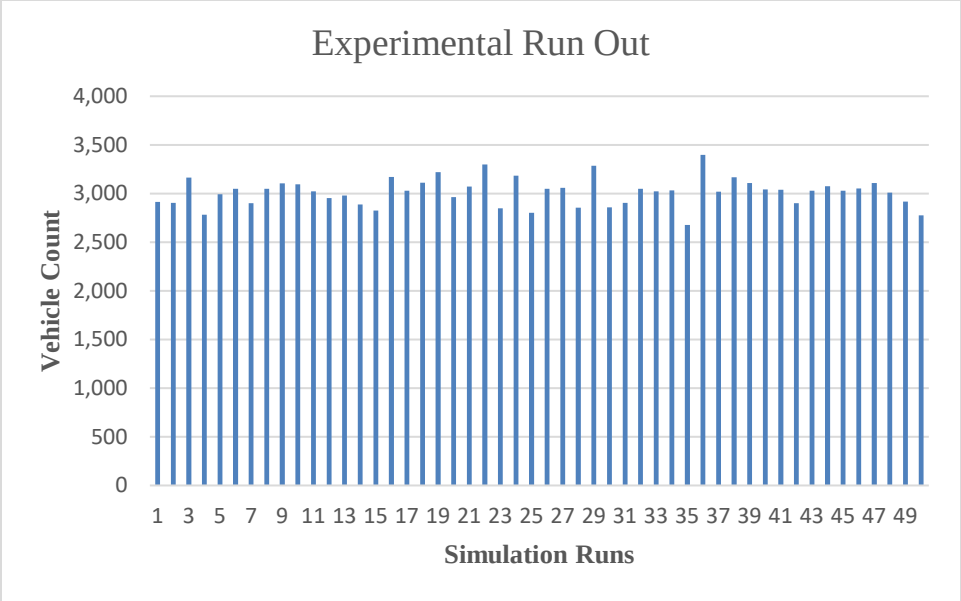

Figure 17. Experimental vehicles running out of gas.

The data required regarding the percentage of vehicles requesting fuel and successfully being served was further analyzed using IBM SPSS software by running the results through one-sample t-tests. The data was found to be significant with a mean of 0.2847 and standard deviation of 0.00016 for the Baseline Percentage and mean of 0.6236 and standard deviation 0.00022 for the Experimental Percentage. The table is attached below:

Table 3. *Vehicles Served Percentage Statistics.*

One-Sample Statistics

	N	Mean	Std. Deviation	Std. Error Mean
Base Percentage	50	.2847	.00016	.0000236
Exp Percentage	50	.6236	.00022	.0000318

One sample statistics of baseline vehicles served and experimental vehicles served.

The independent sample t-test indicated that the differences between the percent of vehicles successfully refueled is significantly with $p < .05$. The information in Table 2 represents the null hypothesis rejected.

Table 4. *Vehicles Served Percentage T-test.*

One-Sample Test

	Test Value = 0					
	t	df	Sig. (2-tailed)	Mean Difference	95% Confidence Interval of the Difference	
					Lower	Upper
Base Percentage	12057.889	49	.000	.2847400	.284693	.284787
Exp Percentage	19589.739	49	.000	.6236282	.623564	.623692

One sample t-test of baseline vehicles served and experimental vehicles served.

Additional tests were run to determine the statistics and significance of the number of vehicles that ran out of fuel in each model. The data is illustrated in Table 3 and Table 4 in below.

Table 5. *Running Out of Fuel Statistics.*

One-Sample Statistics

	N	Mean	Std. Deviation	Std. Error Mean
BaseRunOut	50	16217.925	119.052	16.836
ExpRunOut	50	3015.80	141.186	19.967

One sample statistics of baseline and experimental vehicles running out of fuel.

Table 6. *Running Out of Fuel T-test*

One-Sample Test

	Test Value = 0					
	t	df	Sig. (2-tailed)	Mean Difference	95% Confidence Interval of the Difference	
					Lower	Upper
BaseRunOut	963.253	49	.000	16217.925	16184.091	16251.760
ExpRunOut	151.042	49	.000	3015.800	2975.68	3055.92

One sample t-test of baseline and experimental vehicles running out of fuel.

In conclusion, the null hypothesis was rejected and there was difference between baseline model and experiment model in percentage of vehicles successfully refueled. As the result, there was a difference of over twice the number of vehicles being successfully served in the experimental model with an average of 62.36% versus the baseline 28.47%. What's more, in the baseline model, according to the precondition that 30% of cars don't need to refuel, we generated 58.47% successfully passed the test and 16,218 vehicles being terminated in the experiment. On the other hand, the experimental model showed an increase in mean of percentage of vehicles successfully refueled that 92.36% of cars successfully passed the test and only 3016 cars were terminated during the test. Therefore, there was a dramatic difference of 13,202 cars in between baseline and experiment model. There is a problem that the vehicles did not pass the test will have negative impact of the whole evacuation. For example, the abandoned vehicles will block the evacuation route and cause traffic jams. If cars were trapped by traffic jam, the cost of fuel will be increased. Therefore, more and more cars will be abandoned on the highway, which will lead to a worst condition that no one can evacuate during the hurricane season. In addition, traffic jams always increase the temper of drivers. Drivers will get angry and may fight with each other and cause injuries or deaths, which will be the worst condition that less people can evacuate the hurricane.

REFERENCES

1. Florida Department of Transportation (FDOT) Report. (2018). Hurricane Irma's Effect on Florida's Fuel Distribution System and Recommended Improvements.
2. News article : https://weather.com/safety/hurricane/news/2018-09-11-florence-evacuation-orders-states
3. News article: https://www.floridatoday.com/story/weather/hurricanes/2018/10/09/hurricane-michael-evacuations-residents-urged-leave/1574890002/
4. Cheng, G., Wilmot, C., & E. Baker. (2008). A destination choice model for hurricane evacuation. Transportation Research Board 2008 Annual Meeting Online CD-ROM. Washington D.C.
5. News Article:https://www.citylab.com/transportation/2017/09/why-florida-ran-out-of-gas/539541/.
6. Florida Department of Transportation (FDOT). (2018). Hurricane Irma's Effect on Florida's Fuel Distribution System and Recommended Improvements.
7. Traag, Vincent A. PLoS One; San Francisco Vol. 11, Iss. 4, (Apr 2016): e0153539. DOI:10.1371/journal.pone.0153539. Complex Contagion of Campaign Donations.
8. Ferrara, Emilio; Yang, Zeyao. PLoS One; San Francisco Vol. 10, Iss. 11, (Nov 2015): e0142390. DOI:10.1371/journal.pone.0142390. Measuring Emotional Contagion in Social Media.

9. Bearman PS, Moody J (2004) Suicide and friendships among American adolescents. Am J Public Health 94: 89–95.
10. Herrera, Mauricio; Armelini, Guillermo; Salvaj, Erica. PLoS One; San Francisco Vol. 10, Iss. 10, (Oct 2015): e0140891. Understanding Social Contagion in Adoption Processes Using Dynamic Social Networks.
11. Tsvetkova, Milena; Macy, Michael W. PLoS One; San Francisco Vol. 9, Iss. 2, (Feb 2014): e87275. DOI:10.1371/journal.pone.0087275. The Social Contagion of Generosity
12. Towers S, Gomez-Lievano A, Khan M, Mubayi A, Castillo-Chavez C (2015) Contagion in Mass Killings and School Shootings. PLoS ONE 10(7): e0117259. doi: 10.1371/journal.pone.0117259.
13. Fu, Feng; Christakis, Nicholas A; Fowler, James H. Scientific Reports (Nature Publisher Group); London Vol. 7, (Mar 2017): 43634. Dueling biological and social contagions.
14. Towers, Sherry; Afzal, Shehzad; Bernal, Gilbert; Bliss, Nadya; Brown, Shala; et al. PLoS One; San Francisco Vol. 10, Iss. 6, (Jun 2015): e0129179. DOI: 10.1371/journal.pone.0129179. Mass Media and the Contagion of Fear: The Case of Ebola in America.
15. Sprague, Daniel A; House, Thomas. PLoS One; San Francisco Vol. 12, Iss. 7, (Jul 2017): e0180802. DOI:10.1371/journal.pone.0180802. Evidence for complex contagion models of social contagion from observational data.
16. Ball F, Mollison D, Scalia-Tomba G (1997) Epidemics with two levels of mixing. Ann Appl Probab 7: 4689.

17. Watts DJ, Strogatz SH (1998) Collective dynamics of small-world networks. Nature 393: 440442.
18. May RM, Lloyd AL (2001) Infection dynamics on scale-free networks. Phys Rev E 64: 066112.
19. Keeling MJ (1999) The effects of local spatial structure on epidemiological invasions. Proc R Soc B 266: 859–867.
20. Mathematical Epidemiology, F. Brauer, PV Driesseche and J Wu.
21. Zhang, Ying (n.d). Influenza Trend Prediction Using Kalman Filter and Particle Filter. Department of Physics, Carnegie Mellon University.
22. Aral, Sinan; Nicolaides, Christos. Nature Communications; London Vol. 8, (Apr 2017): 14753. DOI:10.1038/ncomms14753. Exercise contagion in a global social network.
23. Gas Buddy website: https://gasbuddy.com/
24. Yang, K., Wang, E., Zhou, K., & Zhou, Y. (2015). Optimal vaccination policy and cost analysis for epidemic control in resource-limited settings. Emerald.
25. Hansen, E., & Day, T. (2010). Optimal control of epidemics with limited resources. Springer.
26. https://www.wsj.com/articles/gasbuddy-app-scores-big-during-florida-fuel-shortage-1504954805
27. Noam Levin; Alex Mark Lechner; Greg Brown, an evaluation of crowdsourced information for assessing the visitation and perceived importance of protected areas. Applied Geography, ISSN: 0143-6228, Vol: 79, Page: 115-126

28. United States Census Bureau, https://factfinder.census.gov/faces/tableservices/jsf/pages/productview.xhtml?pid=ECN_2012_US_00A1&prodType=table
29. Florida Department of Transportation.
30. Costa, P.J, Dunyak, JP, Mohtashemi, M (n.d). Models, Prediction, and Estimation of Outbreak of Infectious Disease. The MITRE Corporation.
31. Sabet MT, Sarhadi P, Zarini M. Extended and Unscented Kalman filters for parameter estimation of an autonomous underwater vehicle. Ocean Engineering. 2014;

APPENDIX

Presentation slides from this project:

Hurricane Evacuation and Fuel Shortage: Modeling and Analysis

Sirish Namilae & Sabique Islam

Collaborators: Dahai Liu, Scott Parr, Richard Prazenica

EMBRY-RIDDLE
Aeronautical University
DAYTONA BEACH, FLORIDA

Acknowledgement: DOT-UTC CATM for research funding

What Happens during Hurricanes: Case study Hurricane Irma?

- Land Fall September 10, 2017.
  - First was near Cudjoe Key in the lower Florida Keys, at 9:10 AM ET as a Category 4 hurricane
- Second at approximately 3:35 PM ET near Marco Island, just south of Naples, FL
- Evacuation orders were issued to about **7 million people** from Florida, Georgia and South Carolina for Hurricane Irma.
- Our Traffic Analysis from FDOT data: About **550,000 cars** actually evacuated from Florida. (For comparison Katrina 430,000 vehicles on road)
- Wide spread Fuel shortages reaching 70%
- People **travel long distances** to avoid hurricane disaster[1].

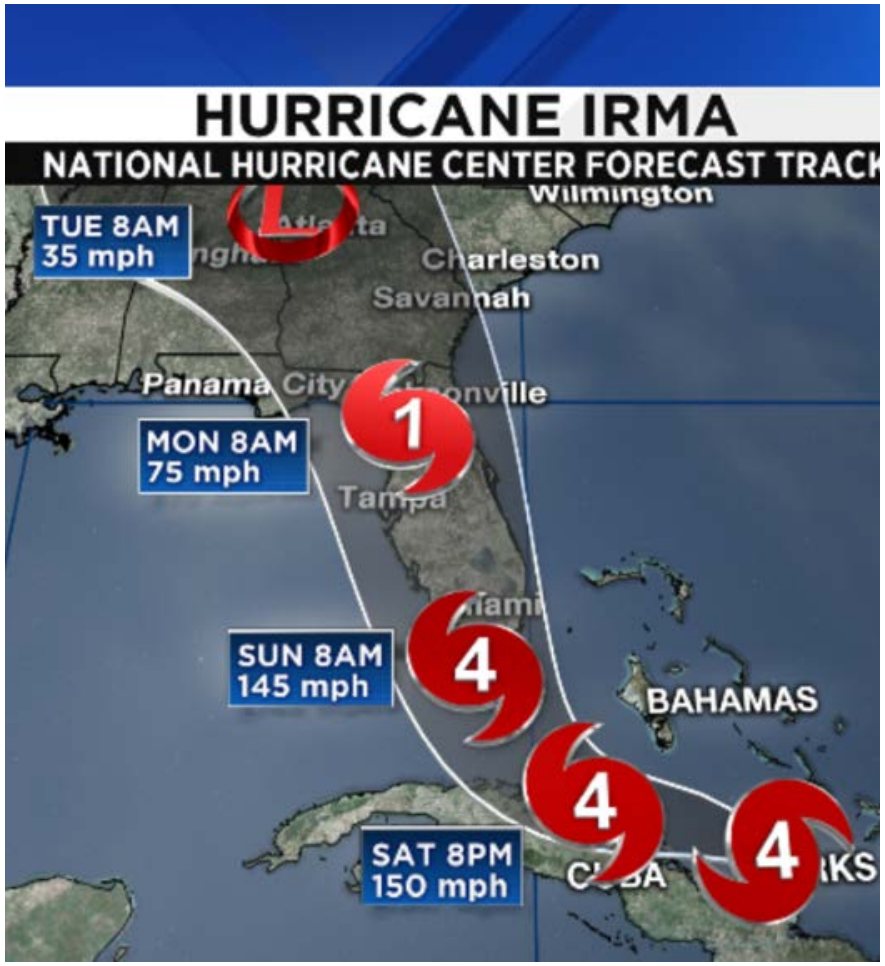

[1]Cheng, G., Wilmot, C., & E. Baker. (2008). A destination choice model for hurricane evacuation. Transportation Research Board 2008 Annual Meeting Online CD-ROM. Washington D.C.

A Closer look at the Traffic – Naples-Fort Myers

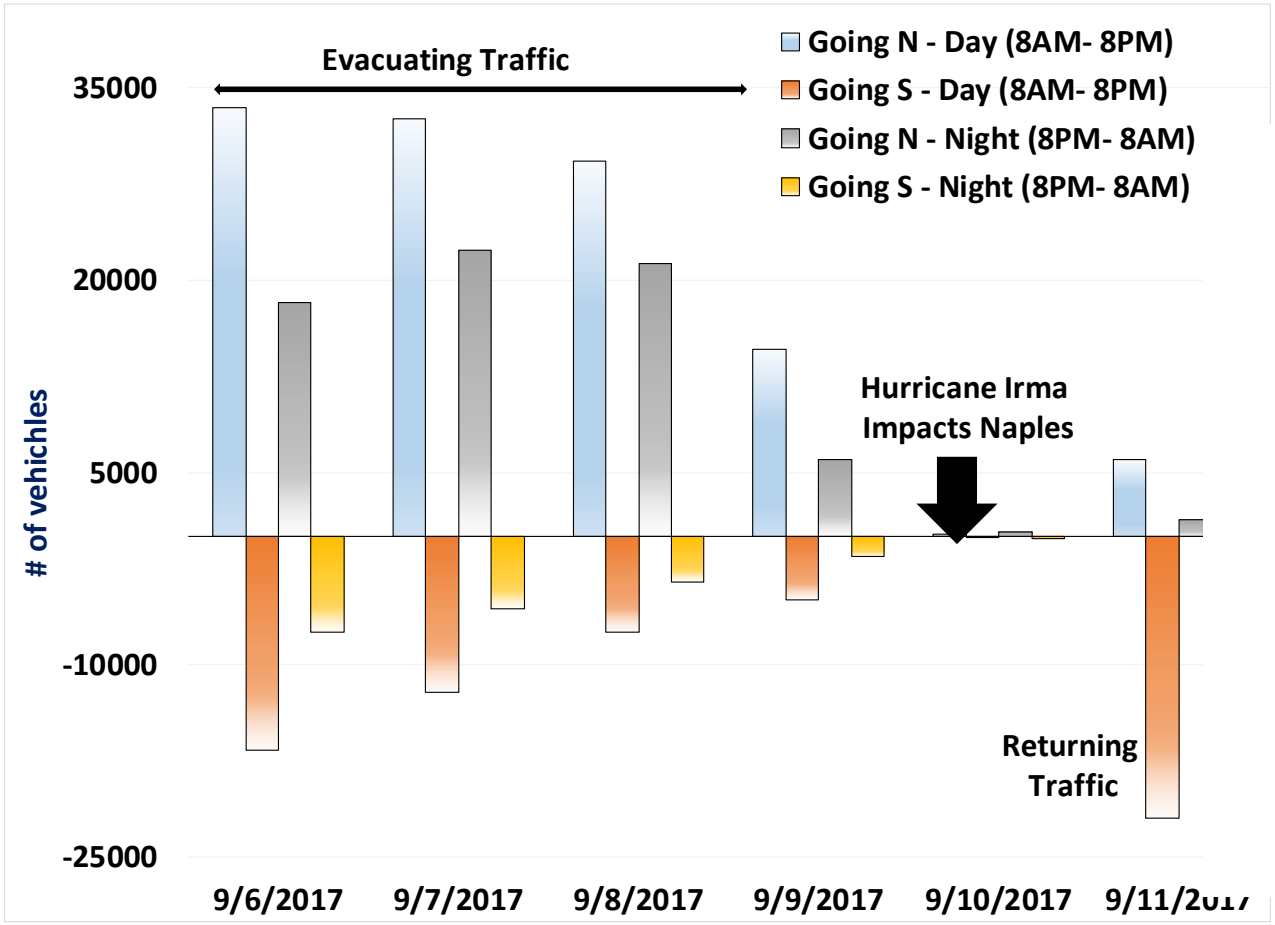

- 7-8 times normal traffic recorded
- Traffic incidents, Fuel shortages and stranded vehicles as a result

Fuel Shortages – Data for Naples-Fort Myers

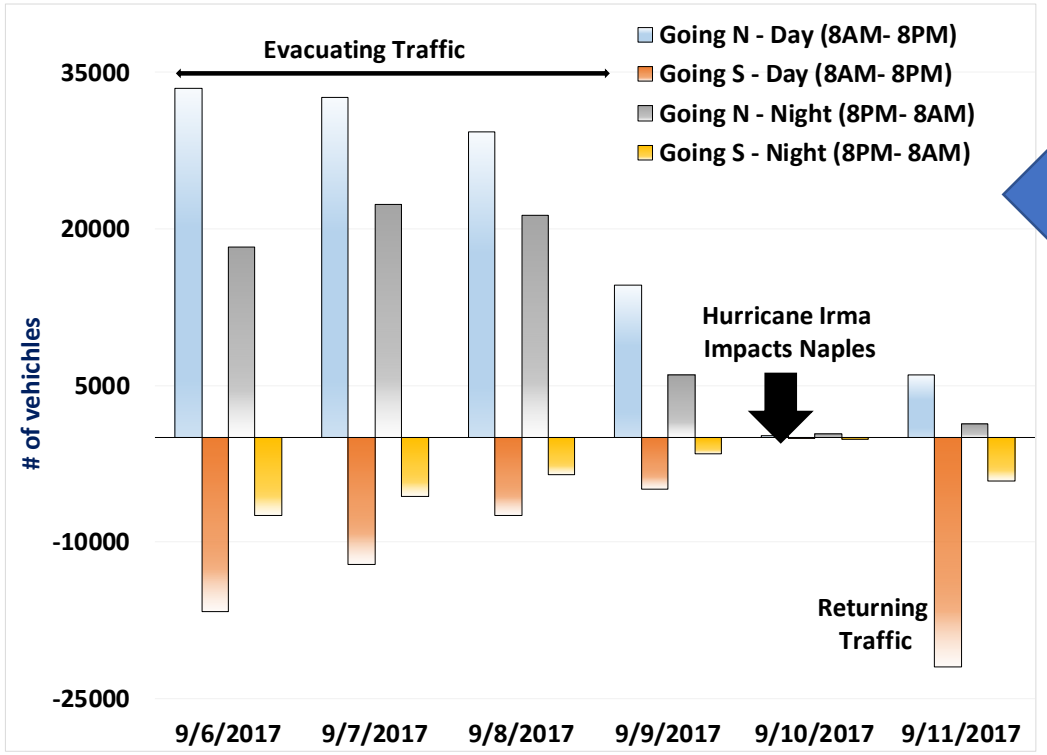

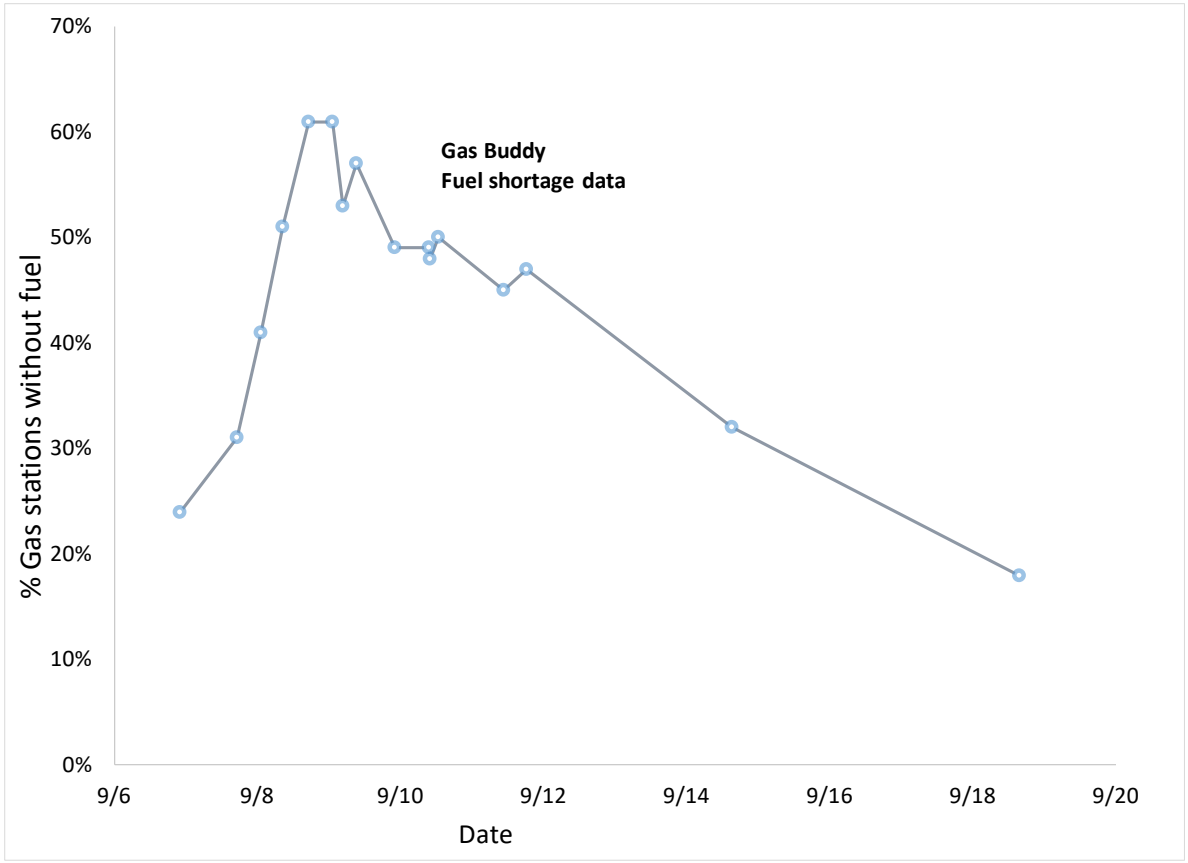

Aggregated data from GasBuddy Clowd source palatform compared with FDOT traffic data

Traffic and Fuel shortages in Tampa- St Petersburg

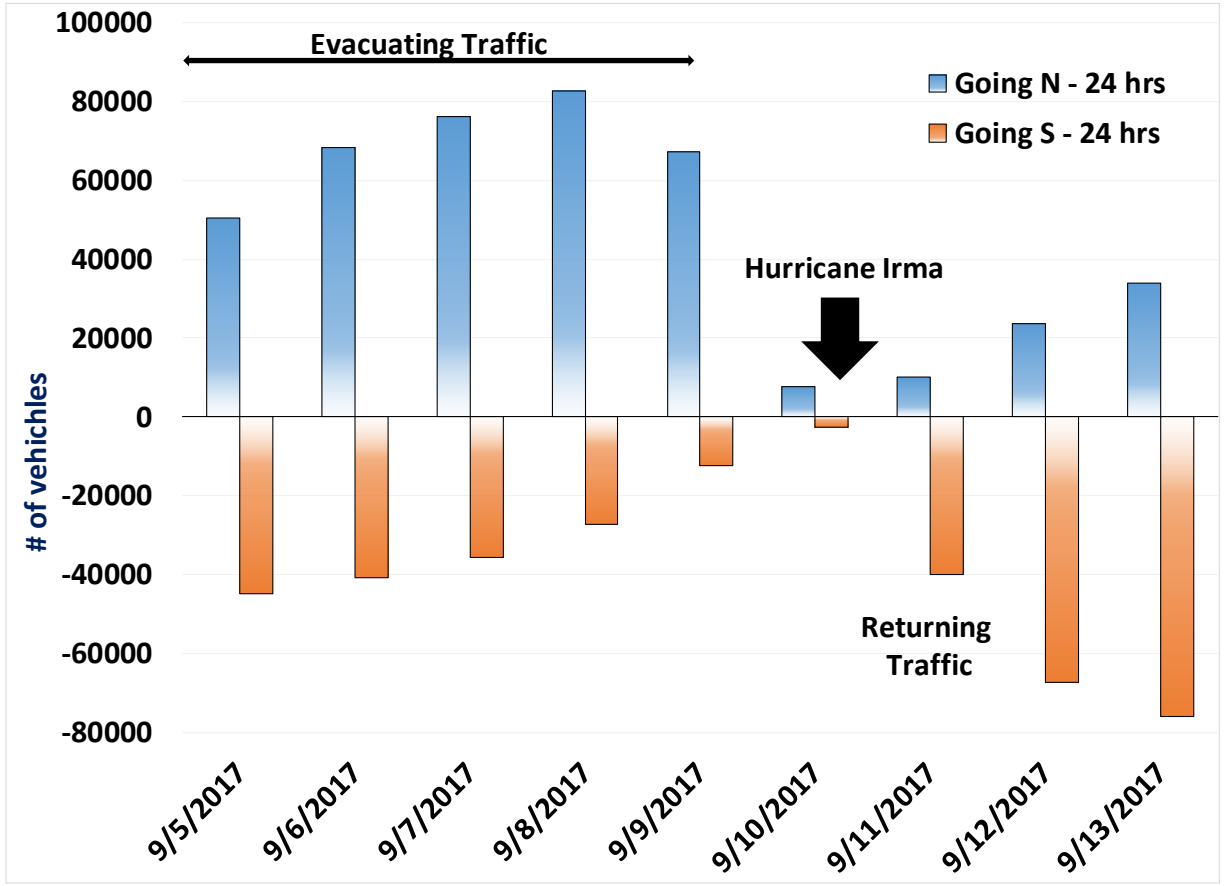

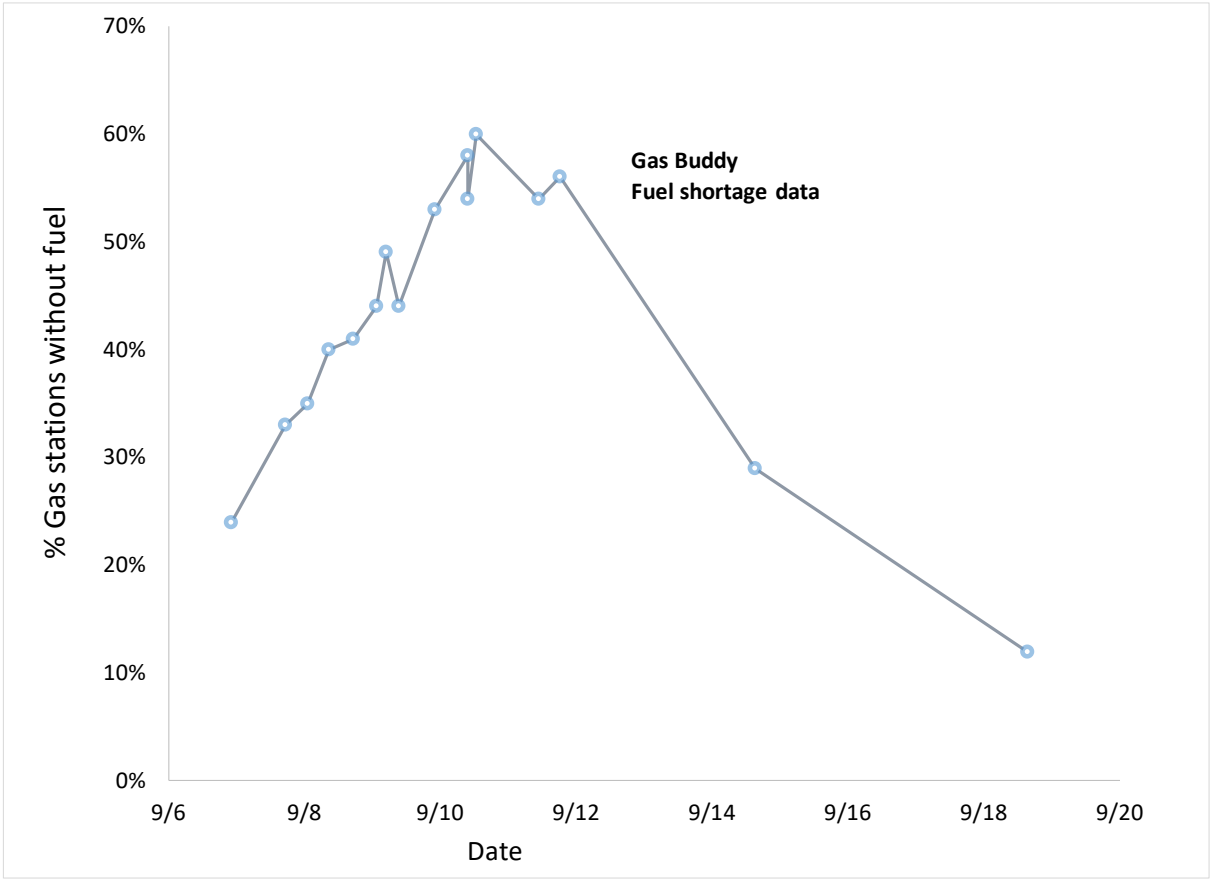

Tampa – St Petersberg – 589,000 vehicles vs 61,000 in Naples
Very simlilar trend as Naples-Fort Myers

Fuel shortages in Miami

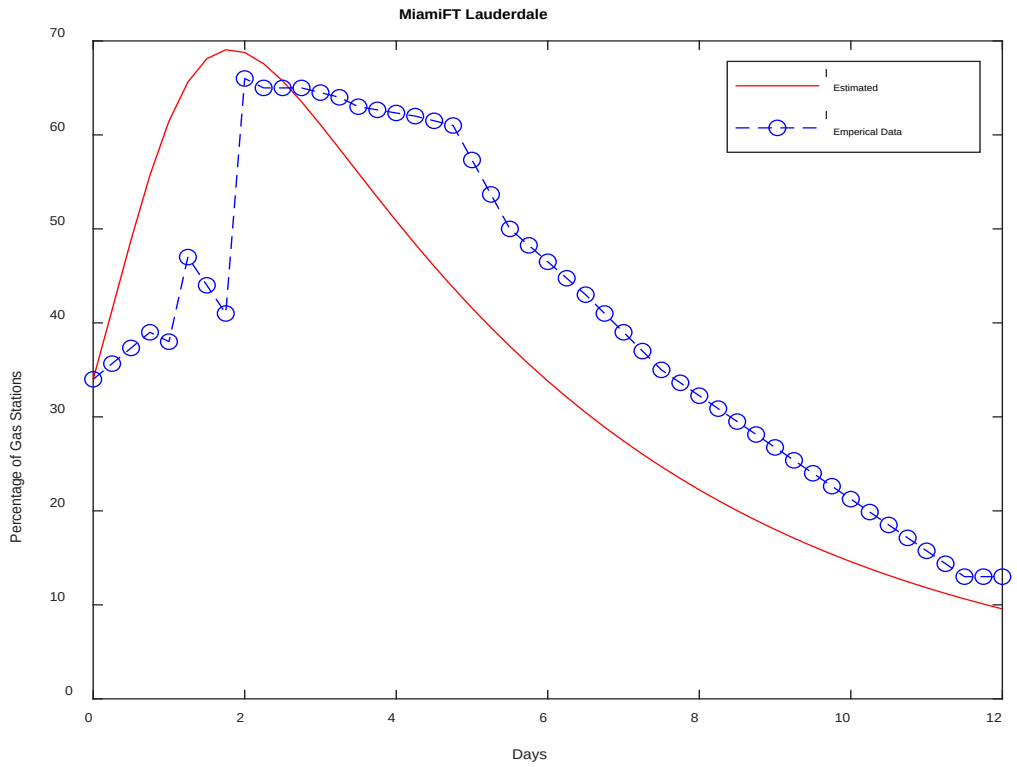

Very simlilar trend of traffic nd fuel shortages in Miami
70% of the 1300 gas stations were out of gas

Florence North Carolina Fuel Shortage Data

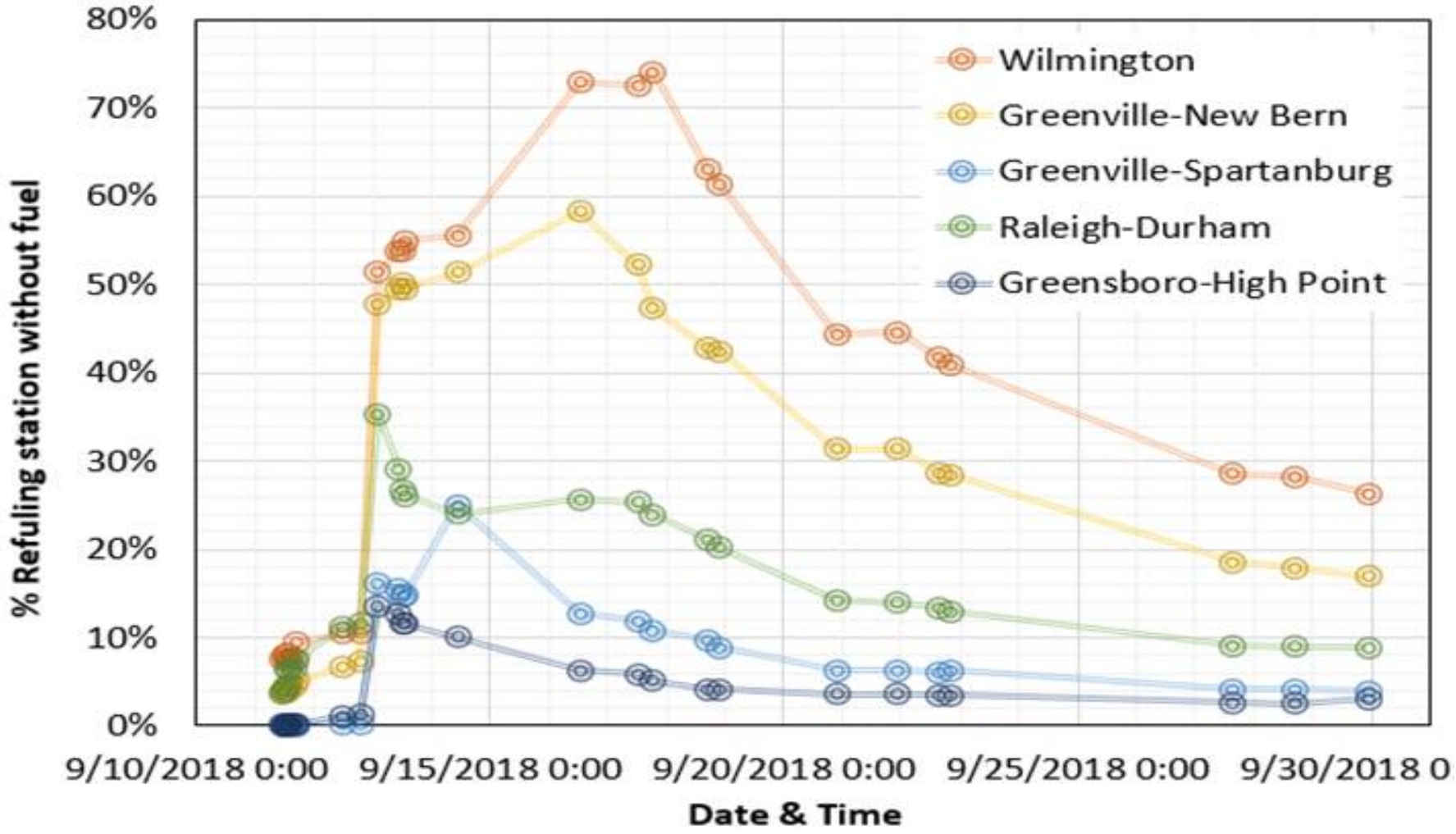

Factors affecting fuel shortage

- **Closure of sea ports** that provide fuel supply
- **Scarcity of fuel supply vehicles**
- **Number of evacuees.**
- **Influx and efflux of traffic** through an area.
- **Initial amount of fuel** in the area

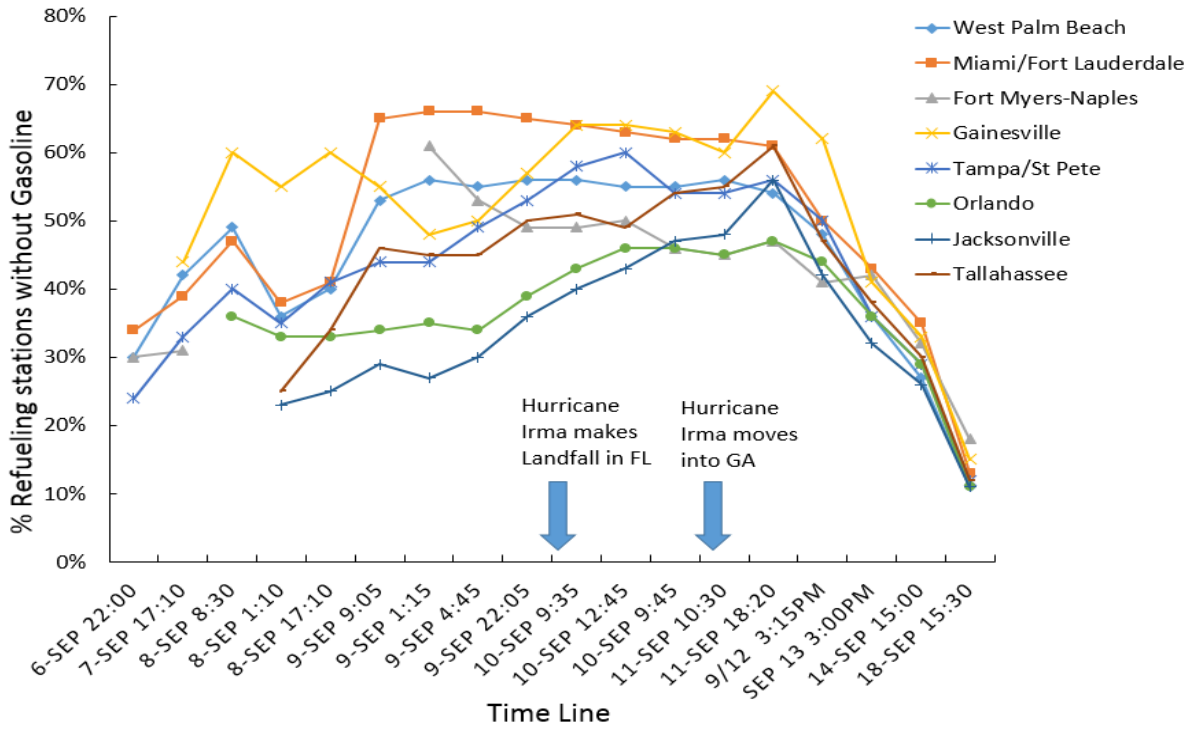

Irma Fuel Shortage Data – All Florida

Ref: Florida Department of Transportation Hurricane Irma Precaution report

Objectives

- Model the hurricane evacuation and related fuel shortage trends
  - Epidemic models and stochastic particle dynamics models
- What factors affect the hurricane evacuation and ensuing fuel shortages
- Can the models be used to predict fuel shortage trends when data starts trickling in early in the Hurricane evolution
- Can the models be used to suggest policy to reduce localized fuel shortages and driver anxiety while increasing overall preparedness

Can we use epidemic models?

Dynamics models of contagious diseases have been effectively used to study problems that exhibit epidemic characteristics.

e.g. Investor panic in financial markets, Contagious effect of mass killings and school shootings

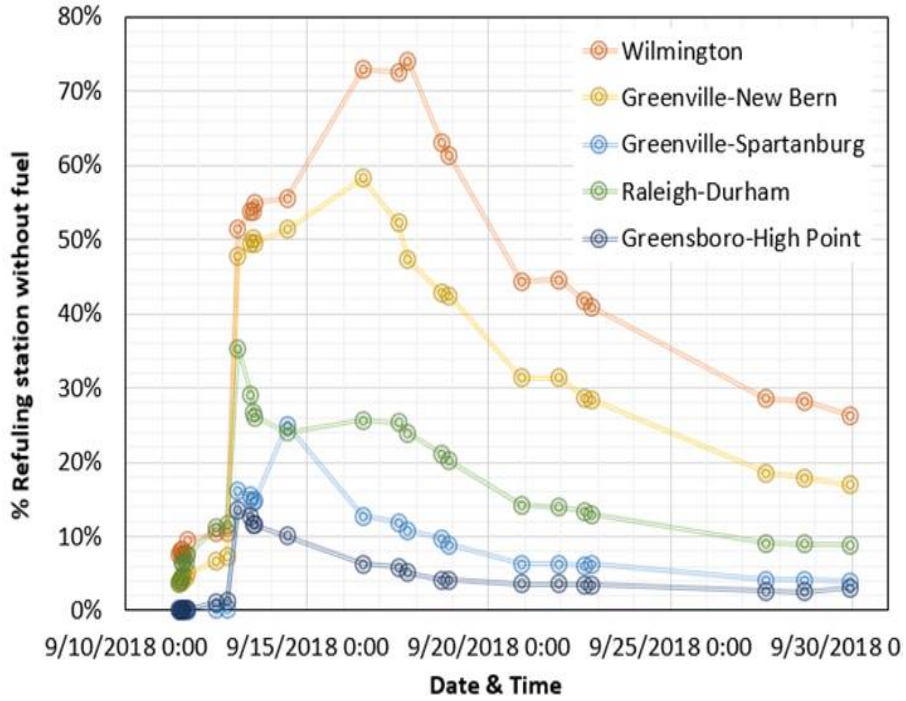

Refueling stations shortage compared to **infections during a flu outbreak** reported by a CDC

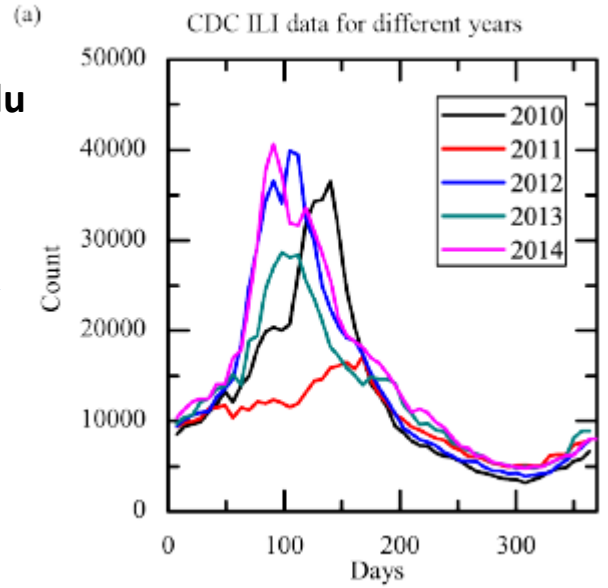

Ref: [1]Shive, S. (2010). An epidemic model of investor behavior. Journal of Financial and Quantitative Analysis, 45(1), 169-198. [2] Towers, S., Gomez-Lievano, A., Khan, M., Mubayi, A., & Castillo-Chavez, C. (2015). Contagion in mass killings and school shootings. PLoS one, 10(7), e0117259.

SIR Disease Dynamics Models

Compartmental epidemic models are based on **dividing the host population into compartments.**

- **Susceptible** – Fuel stations prone to emptying
- **Infectious** –empty and transmitting the pressure of refueling to other fuel stations.
- **Recovered/Removed** – Fuel stations that have been gotten their fuel supply replenished

$$\frac{dS}{dt} = -\beta S(t)I(t)$$

$$\frac{dI}{dt} = \beta S(t)I(t) - \gamma I(t)$$

$$\frac{dR}{dt} = \gamma I(t)$$

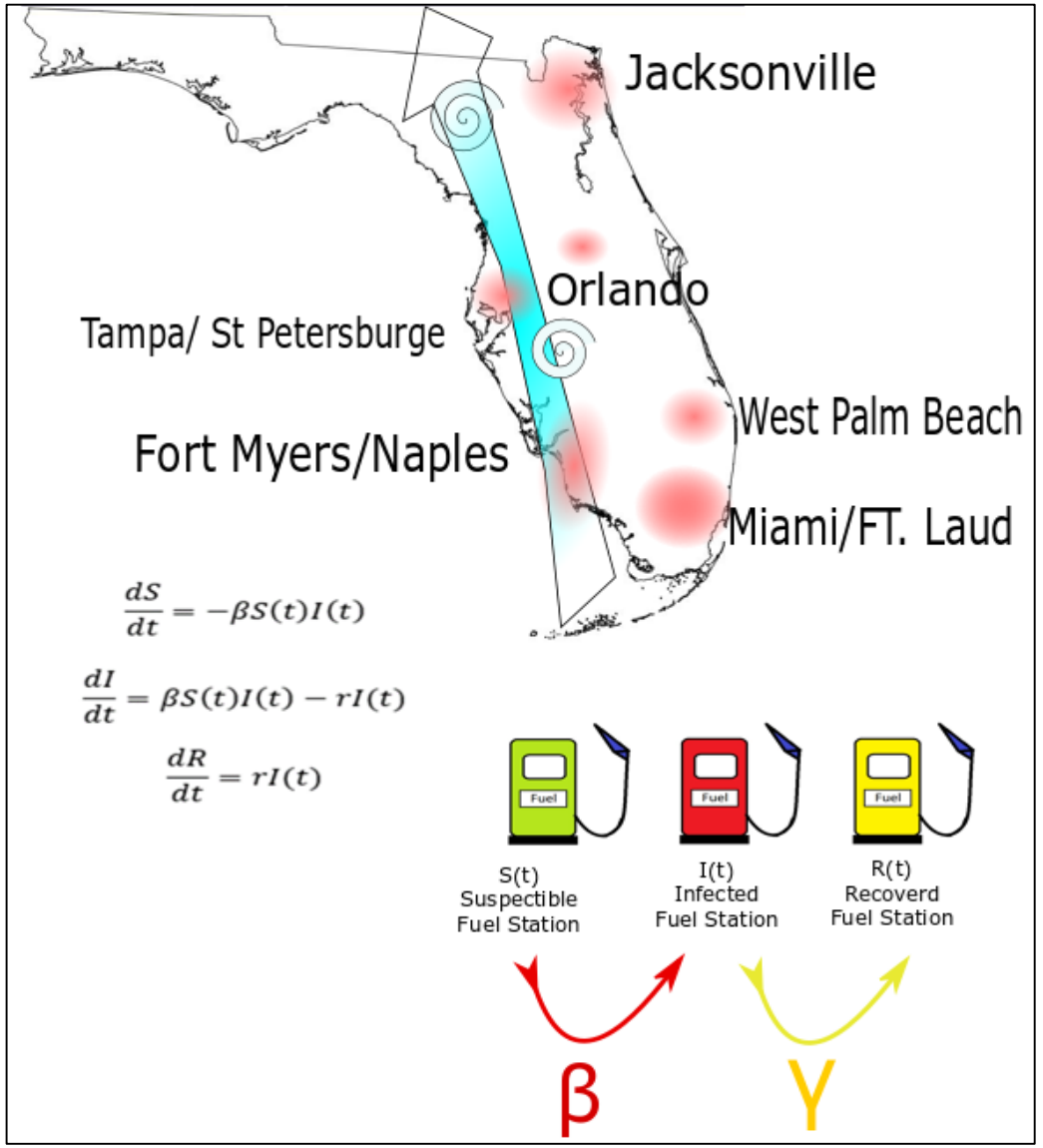

Estimating the SIR Dynamics Parameters

- The parameters β and γ represent the **transmission rate per capita and recovery rate** (so the mean infectious period is $1/\gamma$).
- To determine the β and γ parameters, we used **an Unscented Kalman Filter** was used.
- Another important parameter is Ro – Basic reproduction number

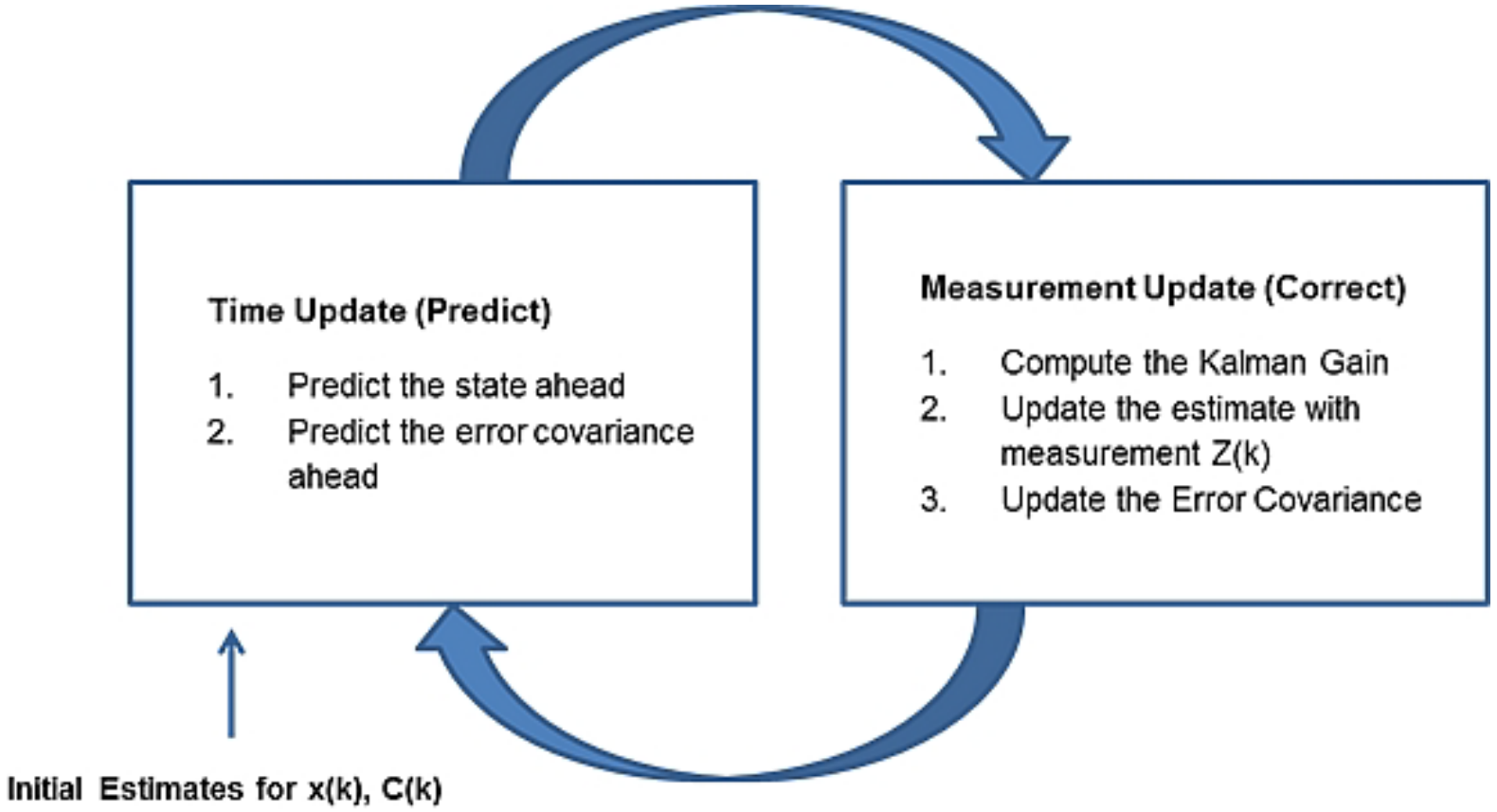

Data for parametrizing the Models

The Data For this study was collected from two sources:

1. The Fuel Shortage Data was obtained from crowd source platform Gasbuddy.com
2. Traffic Data was obtained from FDOT and NCDOT

Ref: Gas buddy Gas Buddy website: https://gasbuddy.com/

Use of the Kalman Filter

- A Kalman Filter is used in various control algorithms, as an observer and sometimes for Parameter Identification for fault tolerance for autonomous systems.

- The Kalman filter uses **sequential observations to estimate the states of the system**. The State Matrix for this problem consists of S(t), I(t), β(t) and γ(t).

- **The UKF (Unscented Kalman Filter) relies on the unscented transformation** and then follows the steps of the KF algorithm.

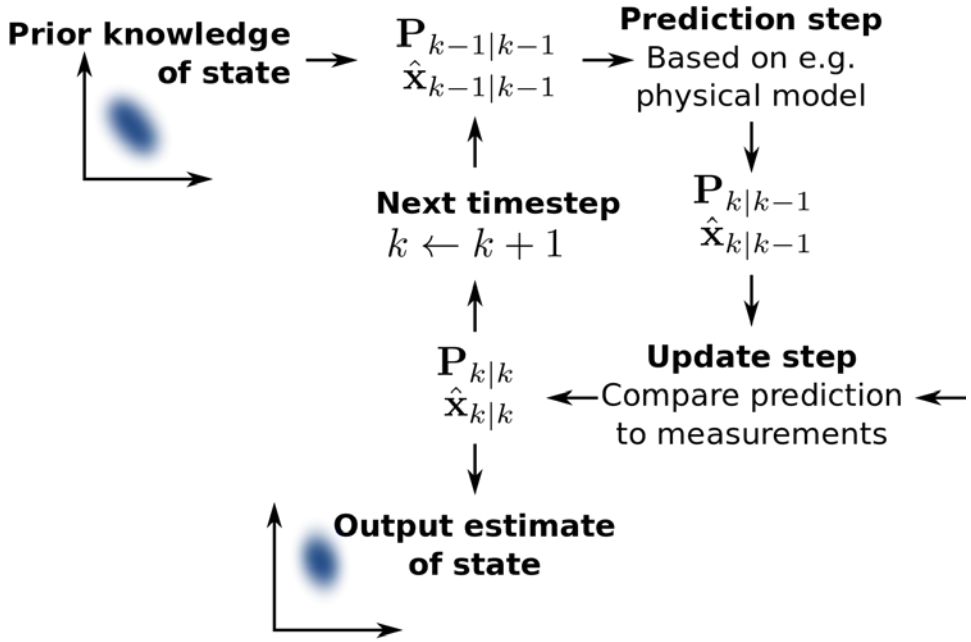

EMBRY-RIDDLE Aeronautical University
DAYTONA BEACH, FLORIDA

Results from the UKF

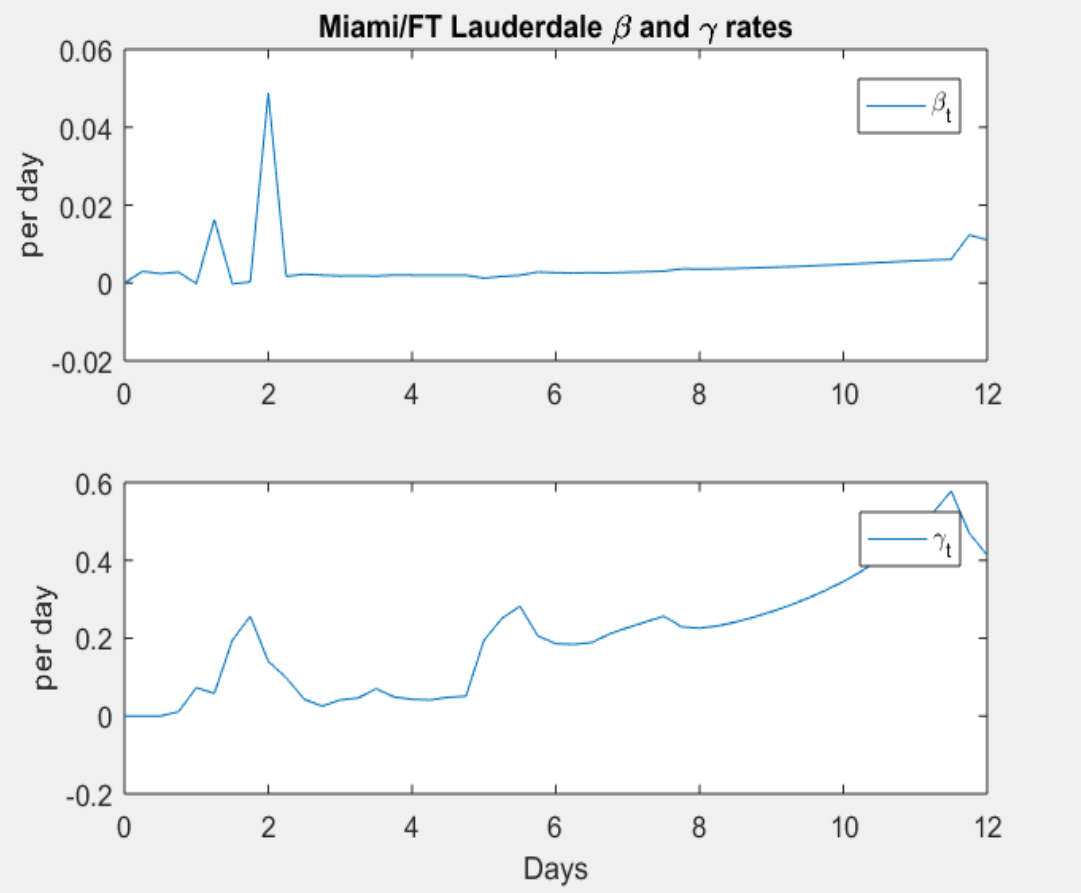

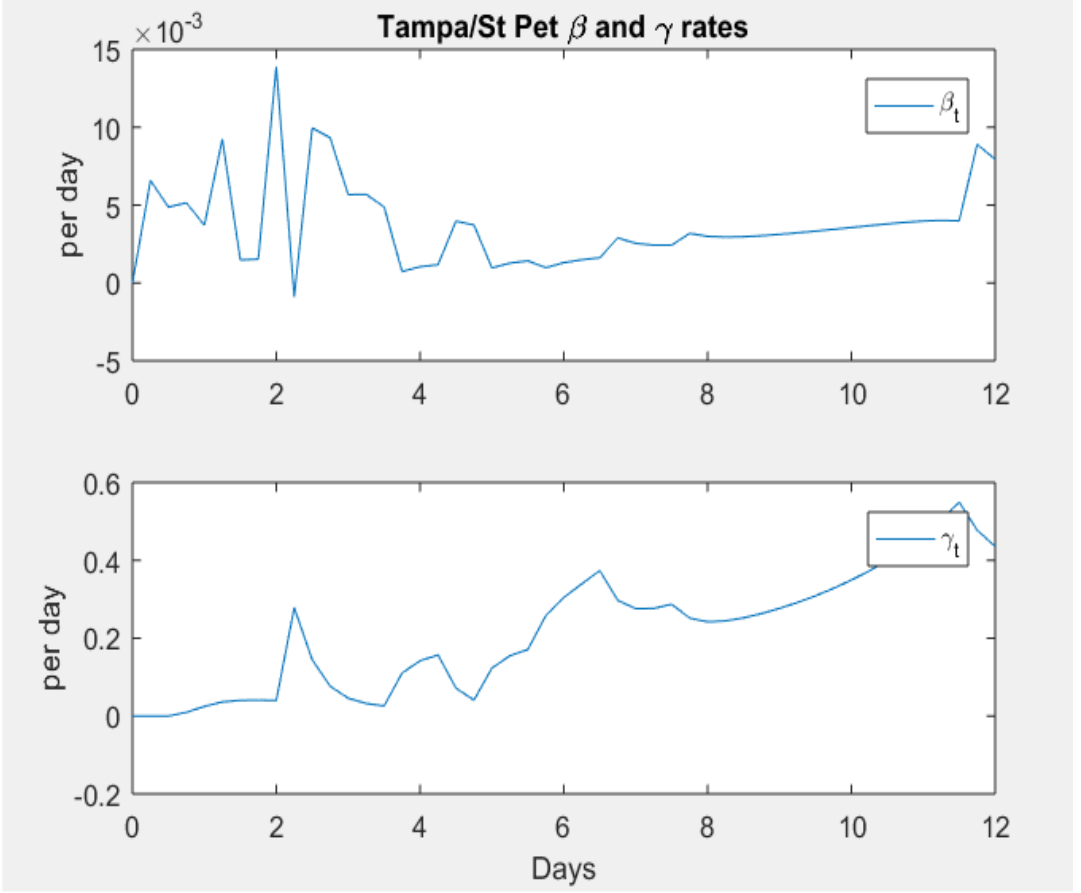

Results from the UKF

City/Area	γ	β	R0	City Area (mi^2)	No. of cars in area	Distance from South
Jacksonville	0.237	0.00969	2.86	874.6	830617	399.23
Orlando	0.210	0.00579	1.93	113.8	270831	276.00
Tampa/St Pete	0.217	0.01389	4.49	312.9	589384	238.00
West Palm Beach	0.200	0.00762	2.67	57.7	89030.00	184.00
Fort Myers-Naples	0.169	0.00887	3.67	65.4	61319	143.00
Miami/Fort Lauderdale	0.206	0.01629	5.54	6137.0	2663214	129.67

Effects of uncertainty

$$R_0 = \beta S(0)/\gamma$$

Similar mean recovery rate estimated

Results and Discussion

Similar infectious period of 5 days observed

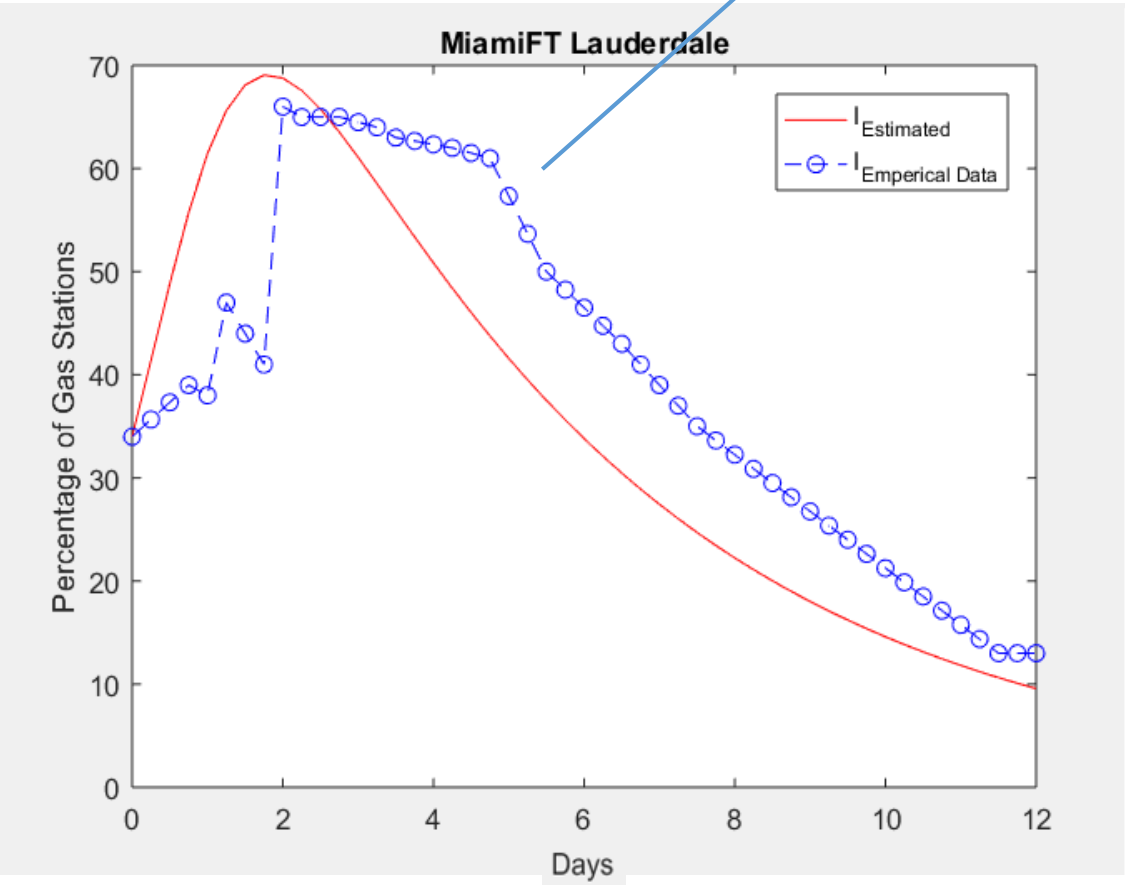

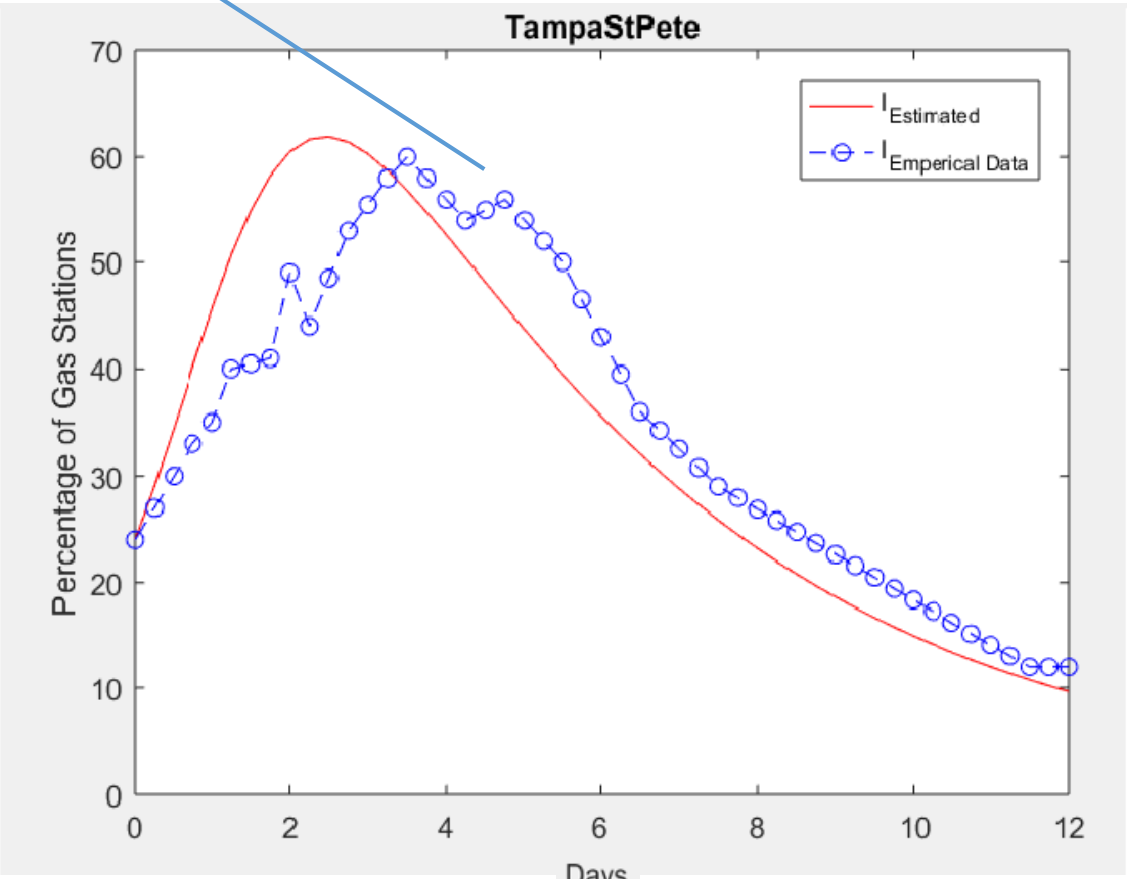

Optimal Refueling Strategy

- Transmission rate (β) and recovery rate (γ) acquired from UKF used to build an augmented SIR model with vaccination policy.
- u_v →rate at which susceptible gas stations are prevented from being emptied by external intervention (extra gas supply).
- Using Bang-Bang Optimal Control Theory, a optimal control algorithm was developed to determine the switching time till which intervention is needed to maximize the effect of the intervention

New Dynamics Equations

$$\frac{dS}{dt} = -\beta S(t)I(t) - u_v S(t)$$

$$\frac{dI}{dt} = \beta S(t)I(t) - \gamma I(t)$$

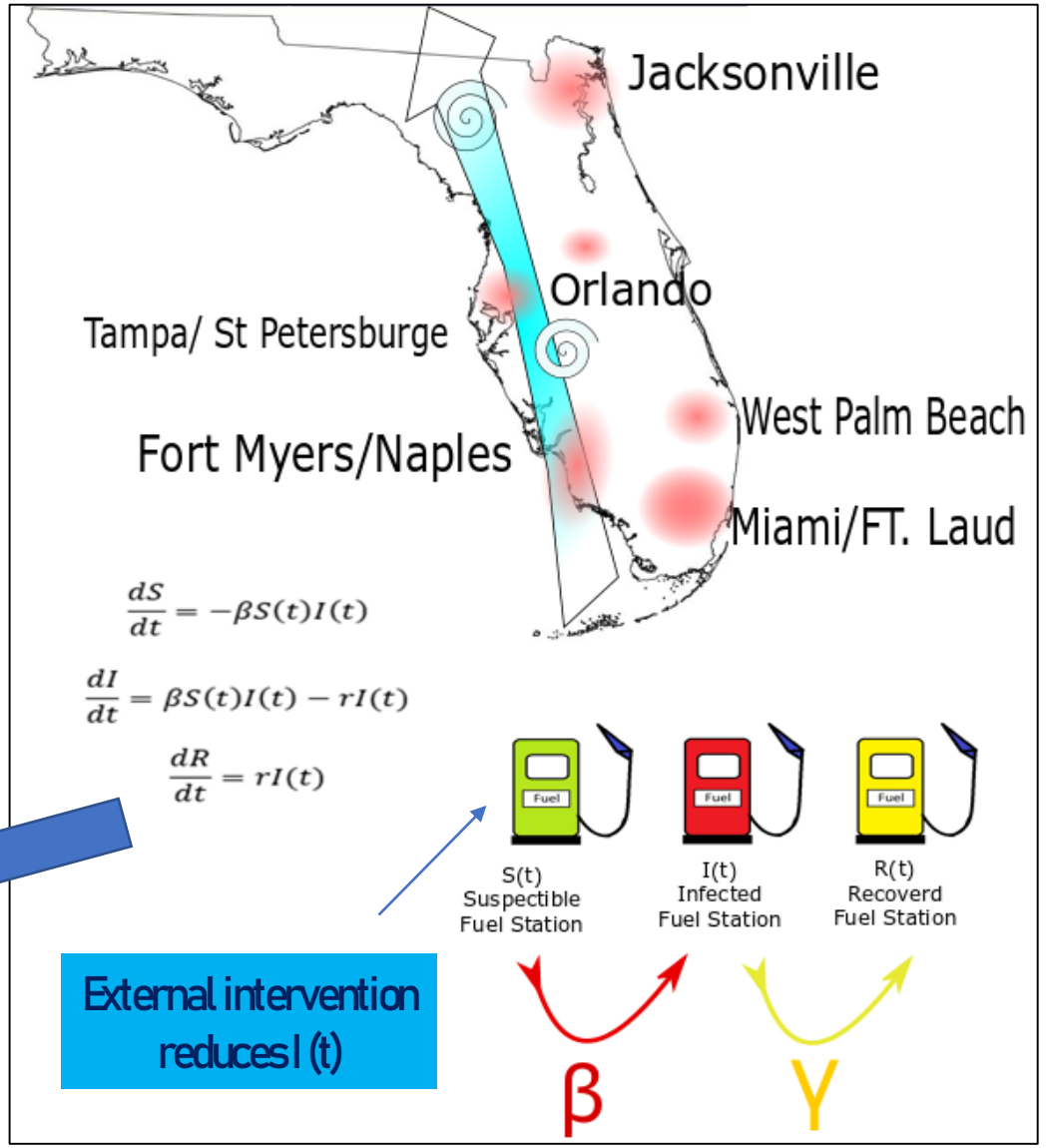

Optimal Refueling Strategy

- Here we apply the control, u_v, for specific time intervals and then switch it "off"
- Optimal control algorithm developed to determine optimal switching time for different intervention levels
- This reduces the fuel shortage problems to acceptable levels
- Below plots show model application to Miami/Ft Lauderdale area.

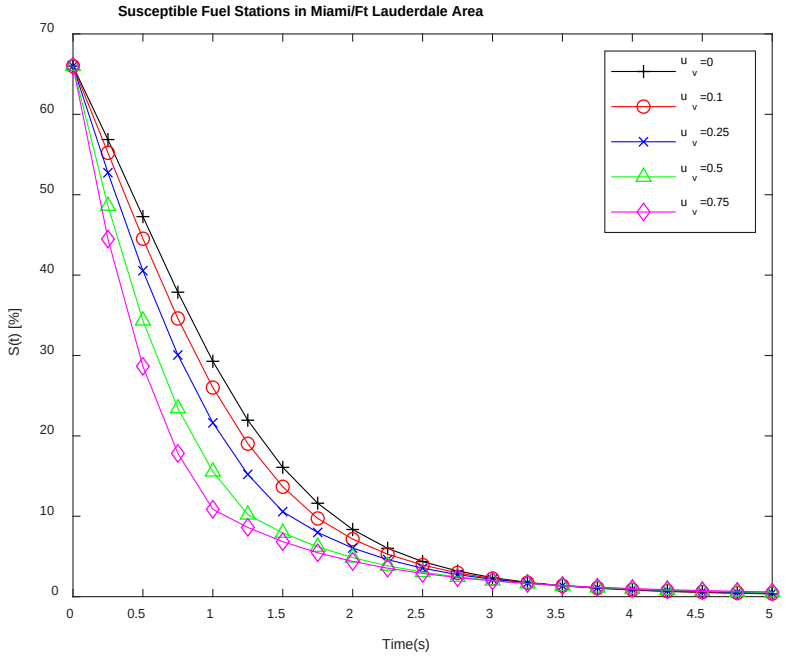

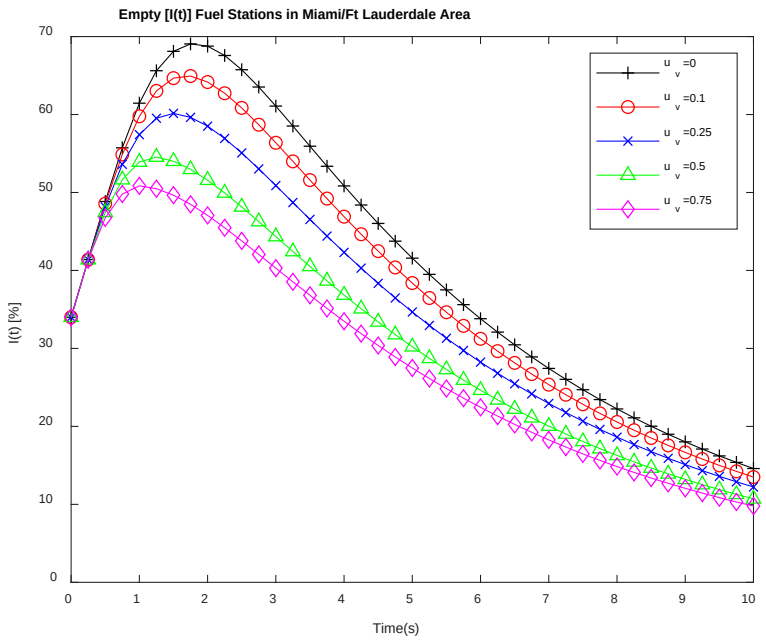

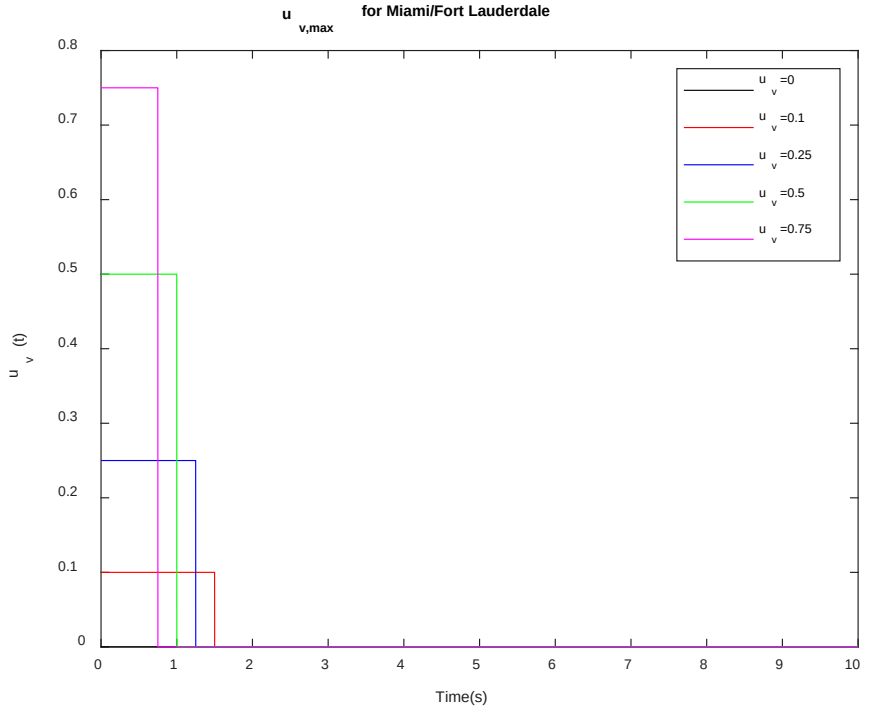

Refueling Strategy for Miami/Ft-Lauderdale

- The maximum percentage of empty fuel stations were reduced to 65% with u_v=0.1. , compared to the base value (when u_v=0) of 70%.
- With the control variable ($u_{v,max}$), the maximum number of infective/empty fuel stations is delayed.
- At a time t=1 day, in S(t), at per capita rate of refueling ($u_{v,max}$) equal to 0.1, a total of (0.1*S(t=1)*1,369*15,000 gl) 534,115 gallons of fuel will have to supplied to be able to control the fuel shortage problem.
- The amount of extra fuel required for refueling strategy changes every time step as, the number of operational fuel stations, S(t), changes per day.

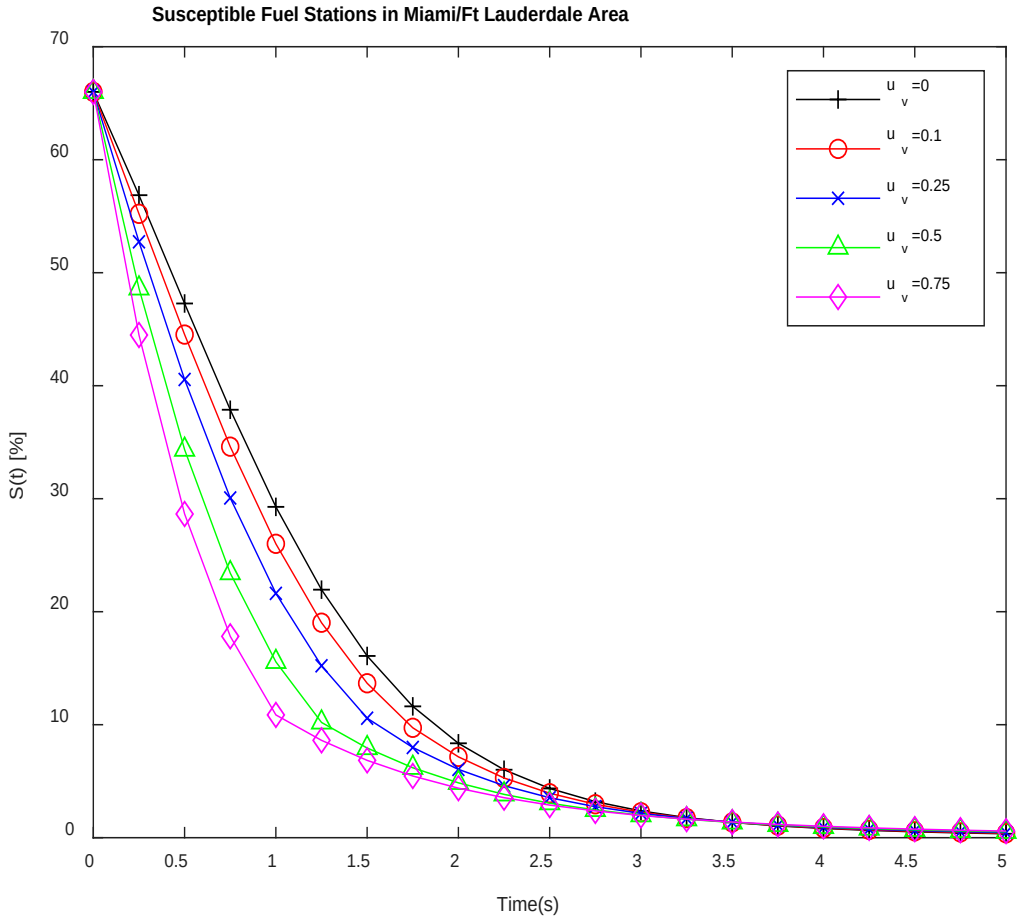

Optimal Refueling Strategy

- In this case the maximum percentage of empty fuel stations were reduced to 65%, for Miami/Ft Laud area compared to the base value of 70% with u_v=0.1.
- It was also observed that with the control variable ($u_{v,max}$), the maximum number of infective/empty fuel stations is delayed.
- As the per capita rate of refueling ($u_{v,max}$) is increased over 0.5, the change in S(t) and I(t) gradually lessens.
- The refueling rate ($u_{v,max}$) is applied from t=0 and then switched to zero at the optimal time as determined by Pontryagine's Maximum Principle.

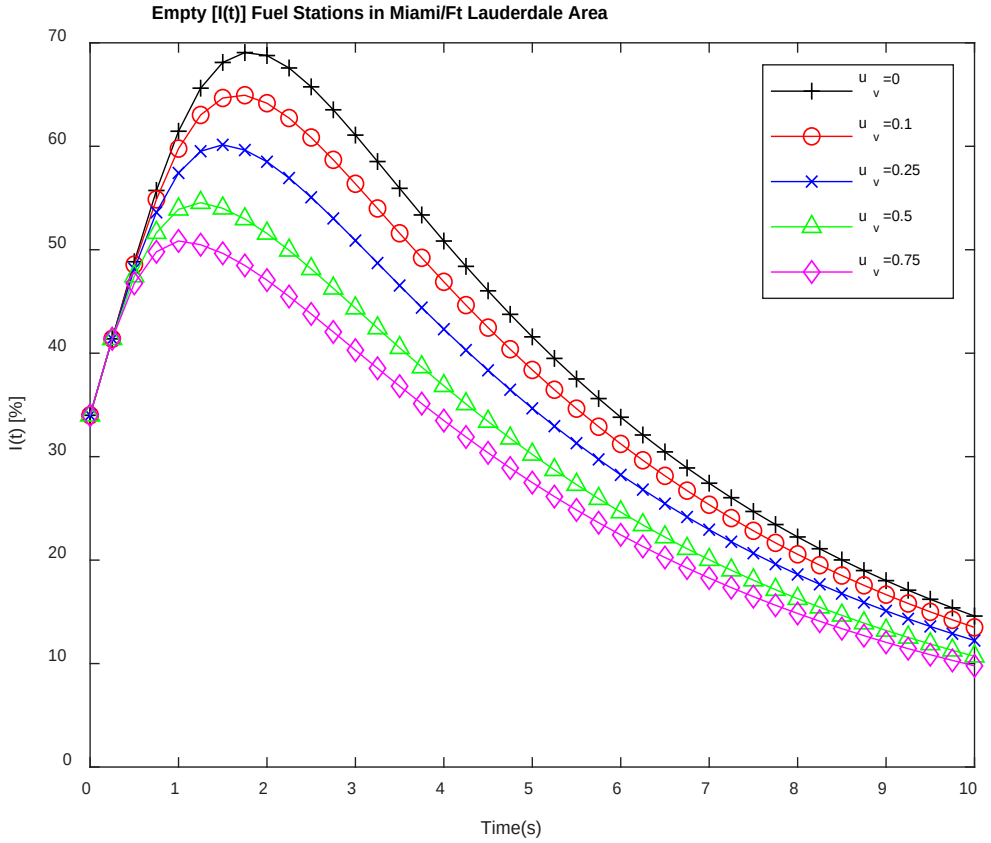

Orlando vs Miami

- The total number of fuel stations in Orlando is 810 (US census).
- At a time t=1 day, A per capita rate of refueling ($u_{v,max}$) = 0.1, a total of (0.1*S(t=1)*810*15,000 gl) 455,625 gallons of fuel is needed to be effective
- This is less then the requirement for Miami/Fort Lauderdale area, and can provide some basis for forming policy.

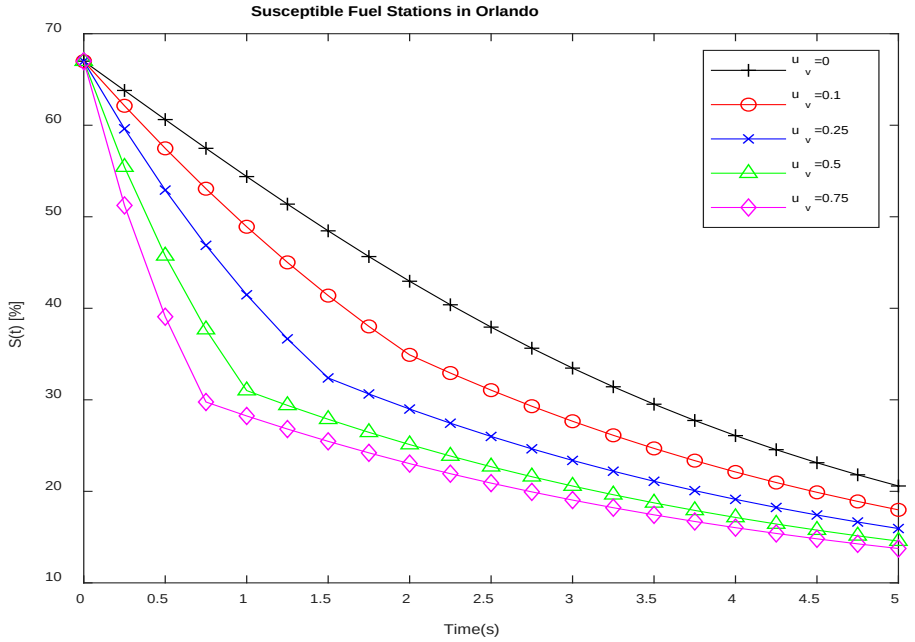

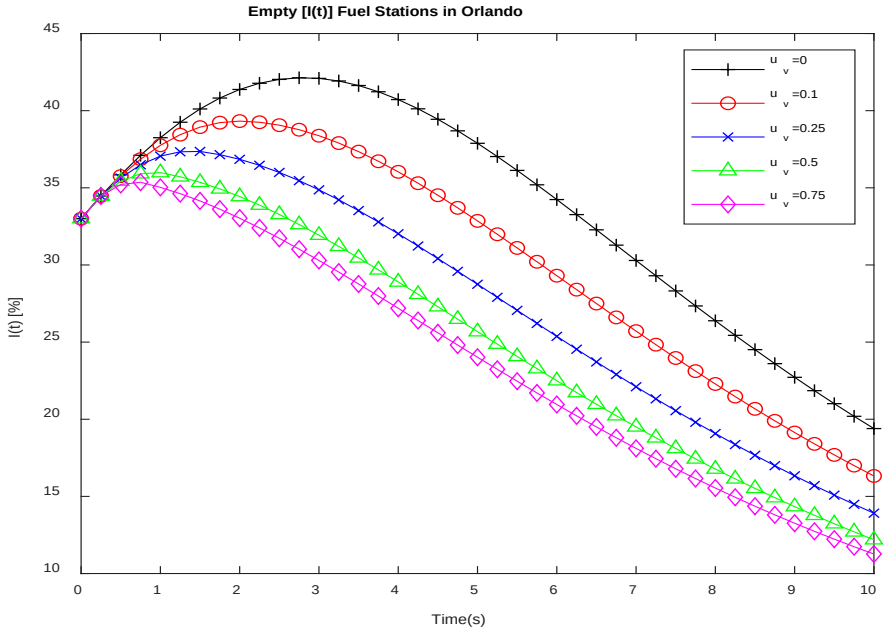

Other Cities affected by Hurricane Irma

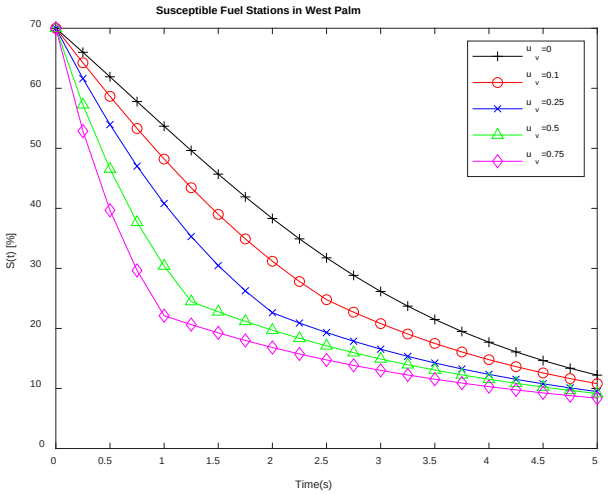

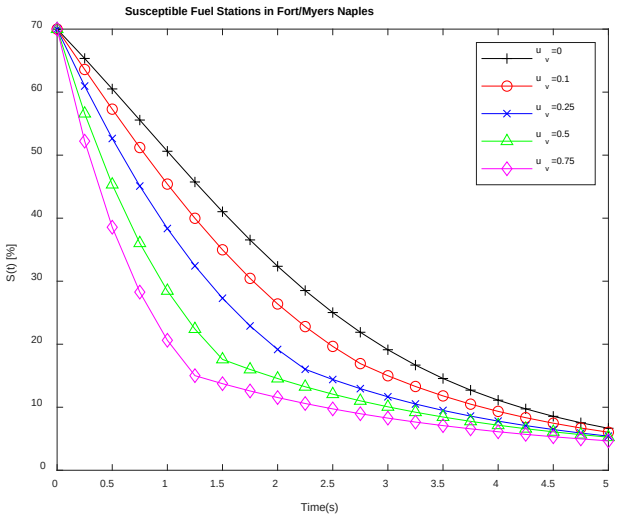

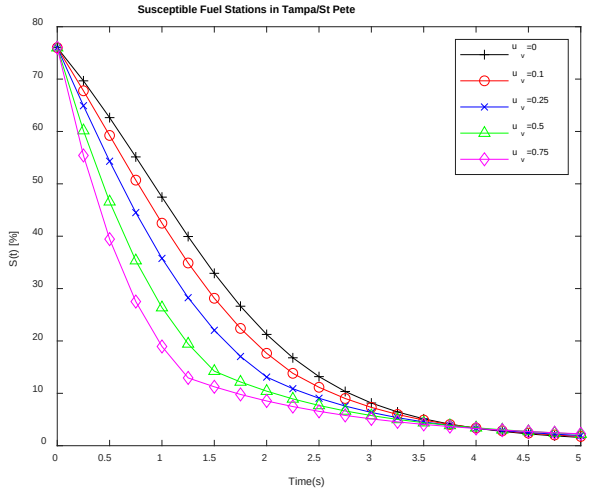

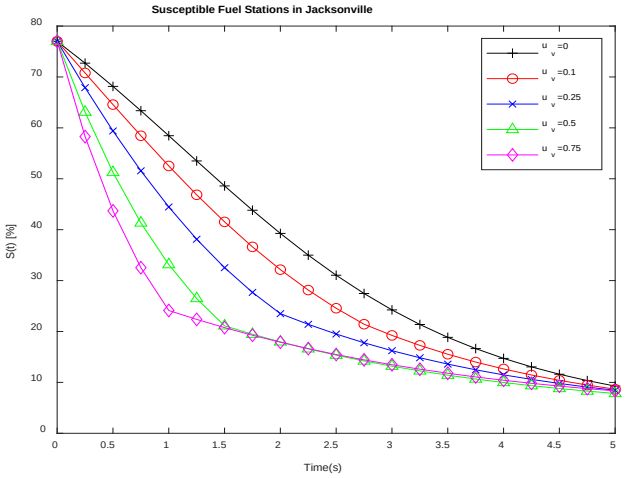

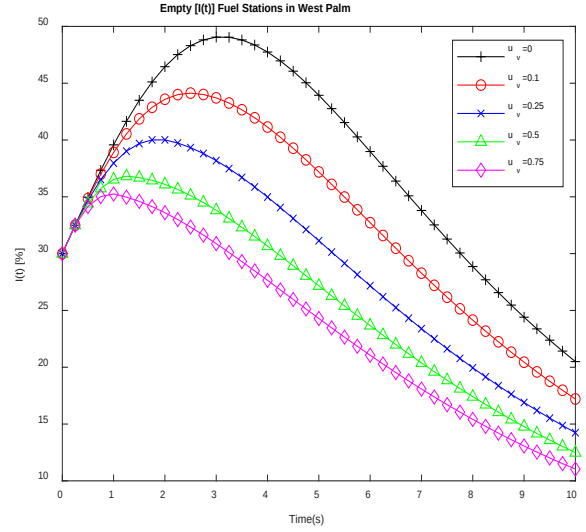

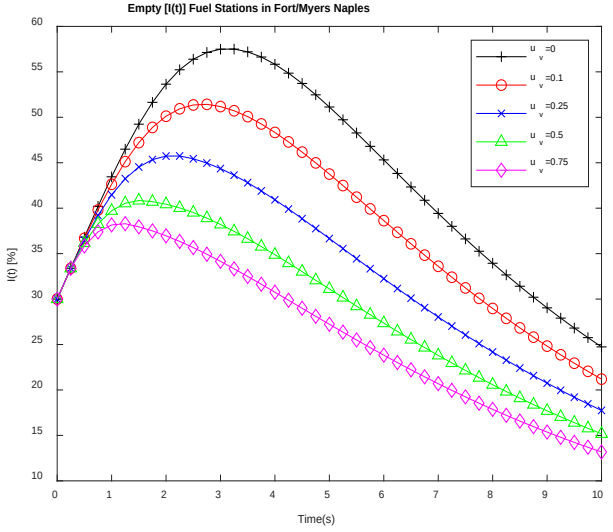

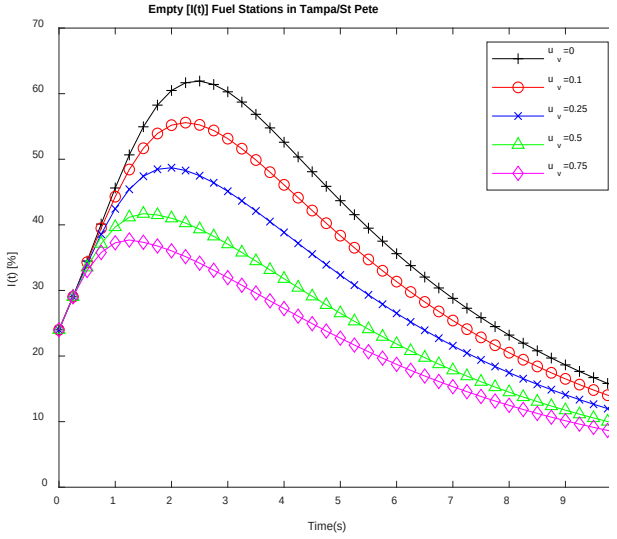

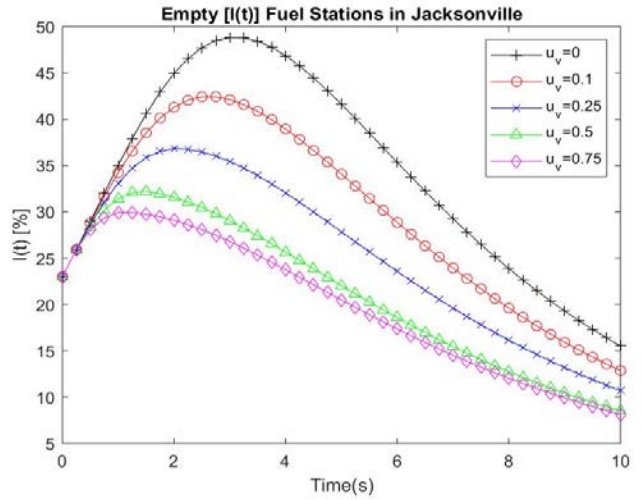

EMBRY-RIDDLE Aeronautical University
DAYTONA BEACH, FLORIDA

Summary

- Hurricane evacuation traffic and corresponding fuel shortage data analyzed
- Fuels shortage modeled as compartmental epidemic model
- The numerical estimation process of Unscented Kalman Filter can be used to prepare better for future hurricanes using present data.
- Optimal control algorithm based on vaccination analogue developed to estimate effective level of intervention

Other ongoing research

Particle Dynamics Traffic Model with Stochastic Fuel Consumption

- Molecular dynamics is a mature simulation method in materials science and chemistry and serves as a framework for our pedestrian dynamics model.

$$\overline{f}_i = \frac{m_i}{\tau}\left(\overline{v}_o^i(t) - \overline{v}^i(t)\right) + \sum_{j \neq i} \overline{f}_{ij}(t)$$

- We introduce location feedback and stochastic fuel consumption rate in that model
  - Velocity altered based on particle in front
  - Fuel level is an evolving variable

$$\overline{v}_o^i(t).\hat{e}_1 = \left(v_A + \gamma_i v_B\right)\left(1 - \frac{\delta}{\overline{r}_i\hat{e}_1 - \overline{r}_k\hat{e}_1}\right)$$

$$fl^i(t) = fl_o^i - \sum_{l=0}^{n} \lambda_{v_l} t_l + R$$

λ_{v_l} is the fuel consumption rate (gallons/hour) at speed of v_l

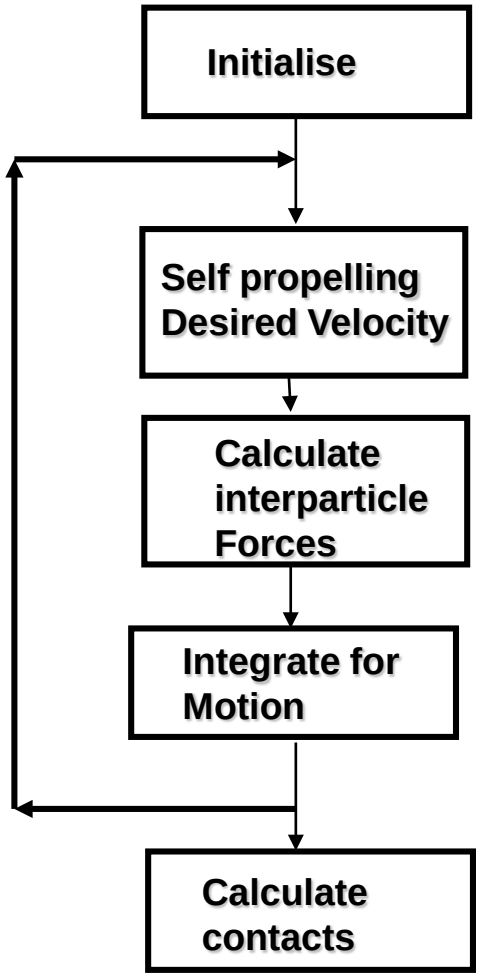

Monte Carlo Fuel Consumption Estimation

- Traffic evolution and stochastic fuel consumption combined with traffic and fuel data
- E.g. Naples-Fort Myers 101 refueling stations→ typical capacity 12000 to 24000 gallons
- Traffic data from FDOT
- Random initial fuel amount + dynamic evolution → Consumption
- Results will be used in policy analysis (Identify critical gas stations) and Self excitation model

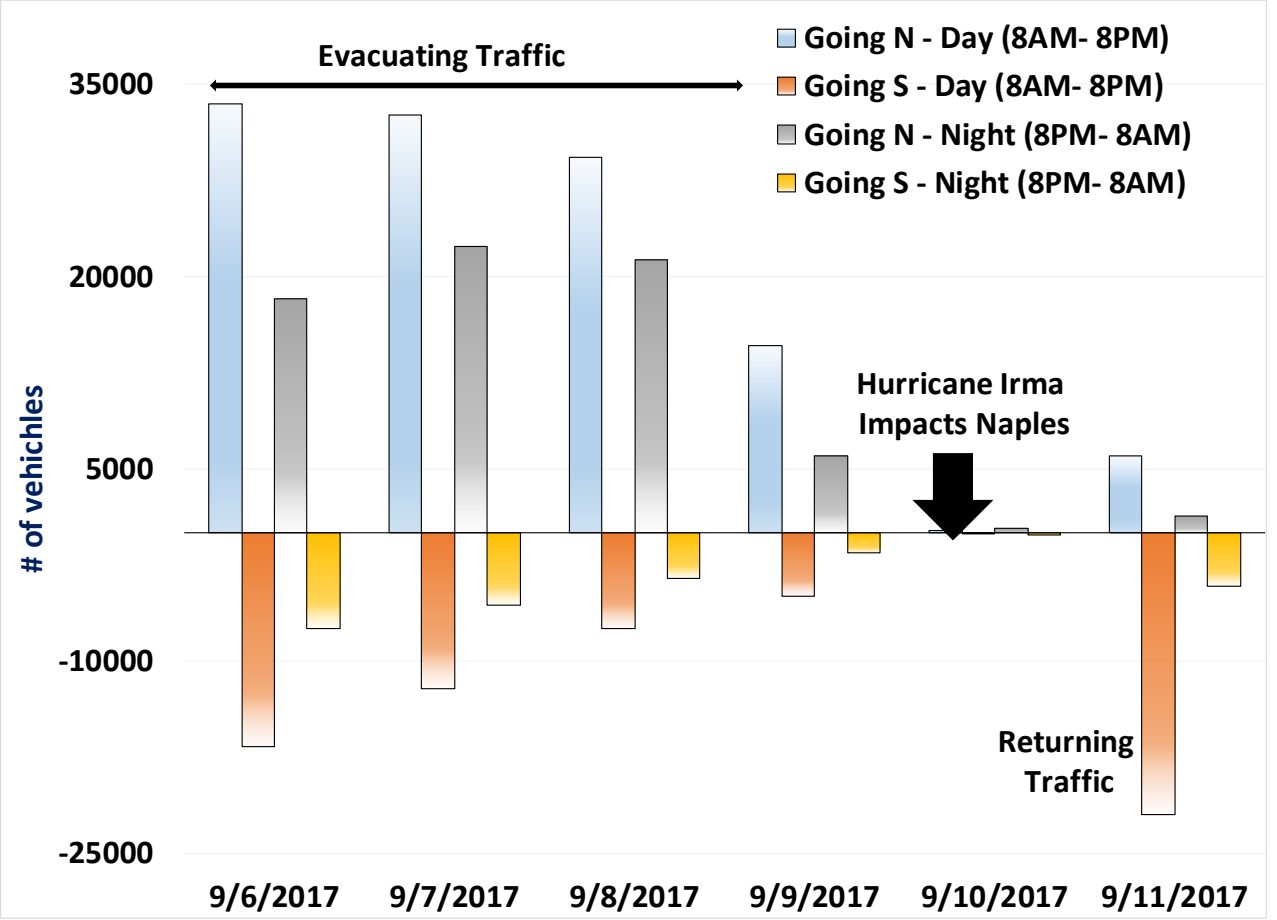

Self Excitation Model

- Self Excitation Model to separate contagious and baseline events. Informs policy analysis
  - Model used in spread of youtube videos, mass shootings, urban crime etc
- Contagion in Fuel shortage due to
  - Excess pressure felt by gas stations when nearby gas station are empty
  - Fuel hoarding by non-evacuees
- conditional intensity function dependent of past events:

$$\lambda(t) = \nu + \sum_{i:t_i<t} g(t - t_i)$$

- *V*→ constant background rate of events &
- *g* → triggering function that determines contagious behavior.
- Monte Carlo Simulation used to assess these different contributions in combination with

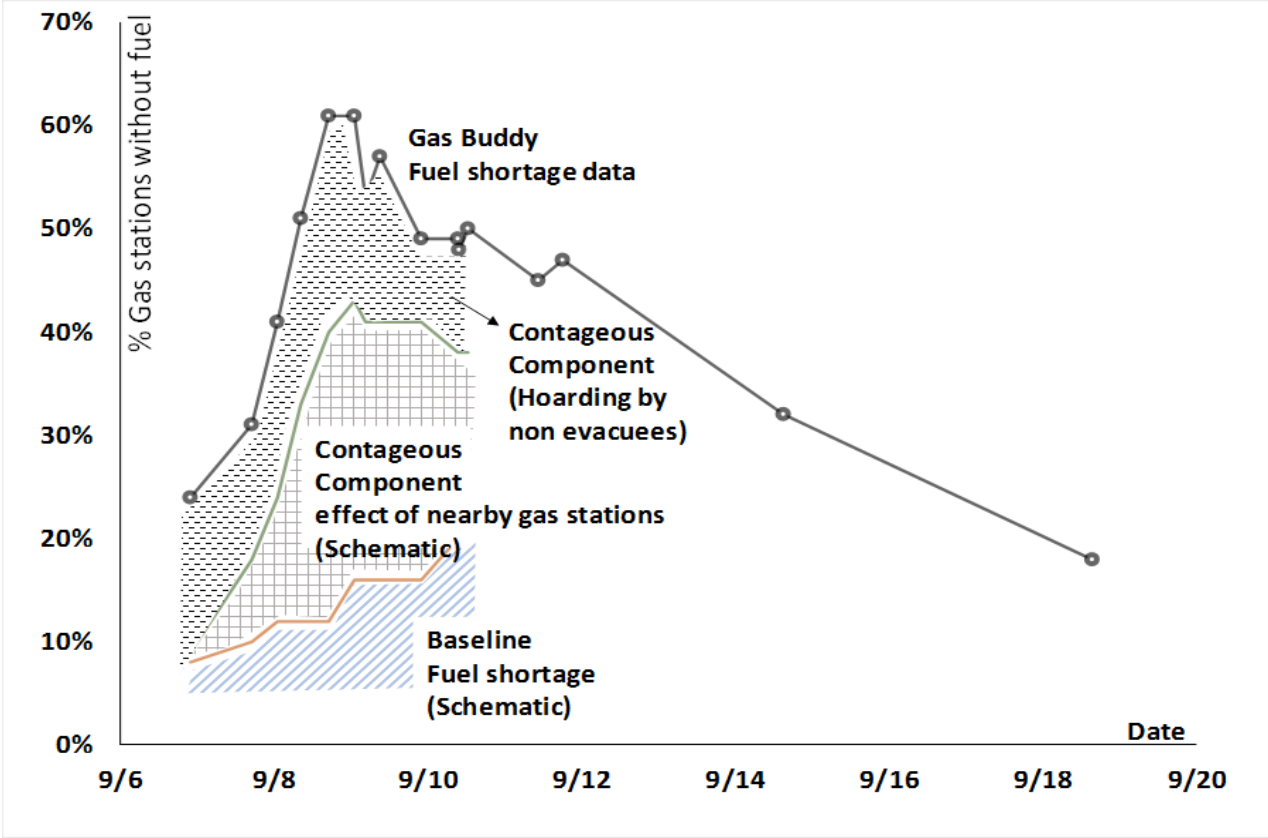

Ref: . Aït-Sahalia, Y., Cacho-Diaz, J., & Laeven, R. J. (2015). Modeling financial contagion using mutually exciting jump processes. Journal of Financial Economics, 117(3), 585-606.

Preliminary Results- Baseline vs Contagion

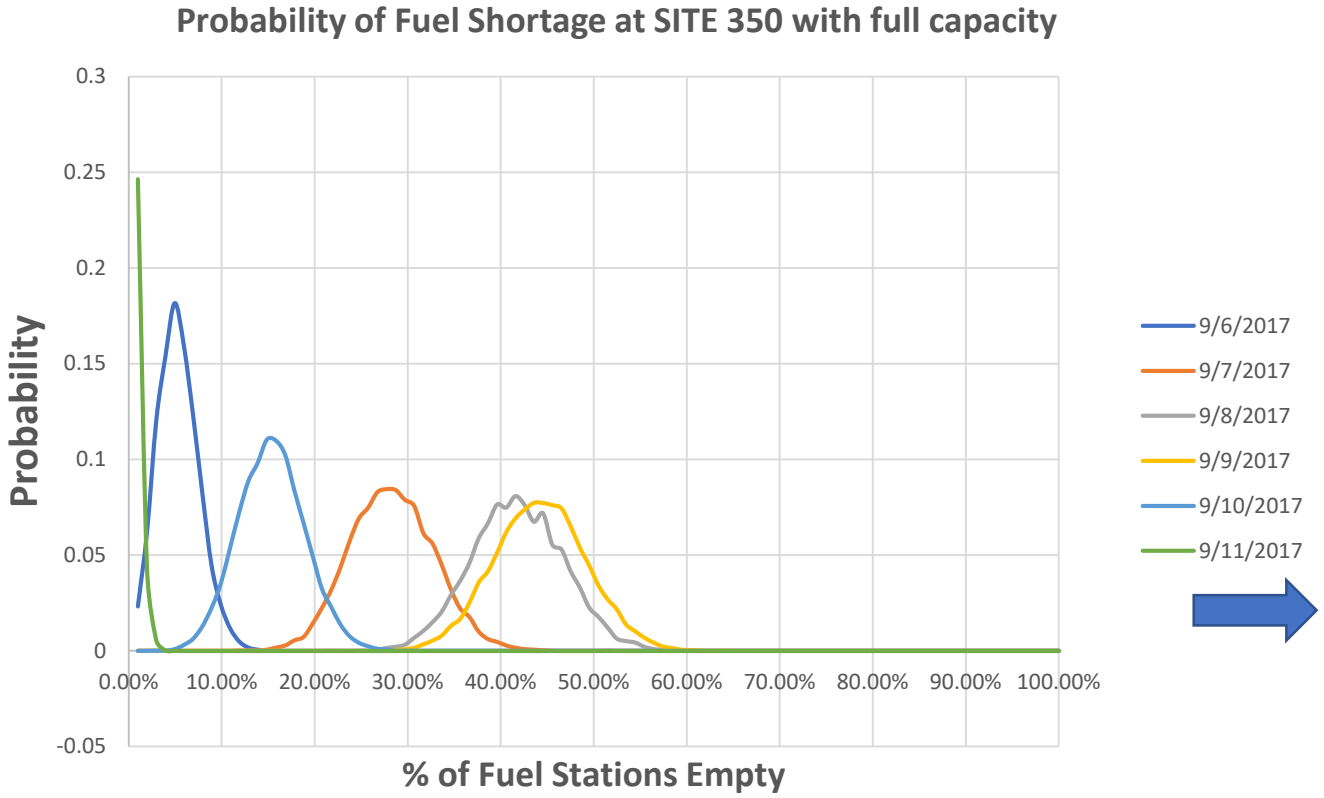

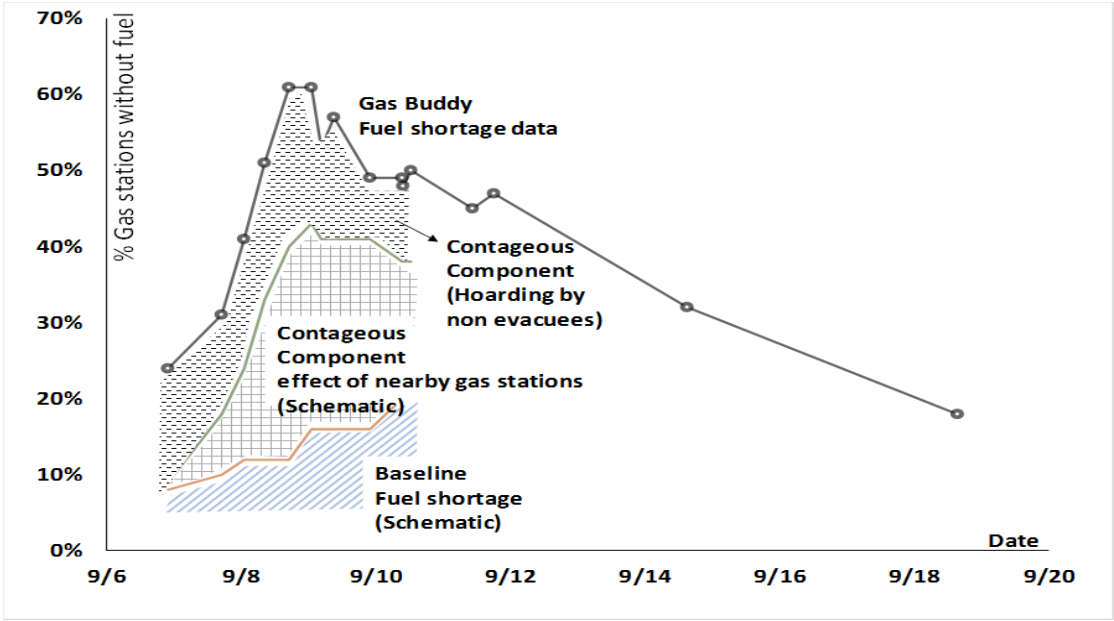

Baseline fuel shortage computed using Monte Carlo model with traffic data from FDOT